Regular Article - Experimental Physics

Limits on the production of the standard model Higgs boson in *pp* collisions at $\sqrt{s} = 7$ TeV with the ATLAS detector

The ATLAS Collaboration[⋆]

CERN, 1211 Geneva 23, Switzerland

Abstract A search for the Standard Model Higgs boson at the Large Hadron Collider (LHC) running at a centre-of-mass energy of 7 TeV is reported, based on a total integrated luminosity of up to 40 pb^{-1} collected by the ATLAS detector in 2010. Several Higgs boson decay channels: $H \to \gamma\gamma$, $H \to ZZ^{(*)} \to \ell\ell\ell\ell$, $H \to ZZ \to \ell\ell\nu\nu$, $H \to ZZ \to \ell\ell qq$, $H \to WW^{(*)} \to \ell\nu\ell\nu$ and $H \to WW \to \ell\nu qq$ (ℓ is e, μ) are combined in a mass range from 110 GeV to 600 GeV. The highest sensitivity is achieved in the mass range between 160 GeV and 170 GeV, where the expected 95% CL exclusion sensitivity is at Higgs boson production cross sections 2.3 times the Standard Model prediction. Upper limits on the cross section for its production are determined. Models with a fourth generation of heavy leptons and quarks with Standard Model-like couplings to the Higgs boson are also investigated and are excluded at 95% CL for a Higgs boson mass in the range from 140 GeV to 185 GeV.

1 Introduction

The search for the Standard Model Higgs boson [1–3] is one of the key aims of the Large Hadron Collider (LHC) at CERN. Prior to the LHC, the best direct information is a lower limit of 114.4 GeV, set using the combined results of the four LEP experiments [4], and an excluded band of 158 GeV to 173 GeV from the combined Tevatron experiments [5, 6]. First results from the ATLAS experiment are available in various Standard Model Higgs boson search channels [7–11]. There are also results from the CMS collaboration [12] in the $H \to WW^{(*)} \to \ell\nu\ell\nu$[1] channel which have a sensitivity similar to the equivalent search reported

here. These results are based on proton-proton collision data collected in 2010 at a centre-of-mass energy of $\sqrt{s} = 7$ TeV. This paper combines the results from the different Higgs boson searches to obtain the overall sensitivity to a Standard Model Higgs boson with the 2010 ATLAS dataset.

All analyses use the most detailed calculations available for the cross sections, as discussed in Sect. 3. The searches in individual Higgs boson decay channels $H \to \gamma\gamma$, $H \to WW^{(*)}$ and $H \to ZZ^{(*)}$ are outlined in Sects. 4, 5, and 6, respectively. The statistical interpretation uses the profile-likelihood ratio [13] as test-statistic. Thirty-one Higgs boson masses, in steps of 10 GeV from 110 GeV to 200 GeV (plus 115 GeV in addition) and 20 GeV from 200 GeV to 600 GeV, are tested. Exclusion limits are obtained using the power constrained CL$_{sb}$ limit [14], as discussed in Sect. 7. To allow for comparisons with the exclusion limits obtained by other experiments, the results are also determined using the CL$_s$ method [15]. The limits are presented in terms of σ/σ_{SM}, the multiple of the expected Standard Model cross section at the Higgs boson mass considered. Results are also presented in terms of the corresponding ratio where the cross section in the denominator includes the effects of a fourth generation of heavy leptons and quarks with Standard Model-like couplings to the Higgs boson. Section 8 describes the treatment of the major sources of systematic uncertainty in the combined likelihood. The limits for individual channels and the combined results are detailed in Sect. 9 and the conclusions are drawn in Sect. 10.

2 The ATLAS detector

The ATLAS experiment [16] is a multipurpose particle physics apparatus with forward-backward symmetric cylindrical geometry covering $|\eta| < 2.5$ for tracks and $|\eta| < 4.5$ for jets.[2] The inner tracking detector (ID) consists of a sili-

---

[1]In this paper, the raised index '*' implies a particle off mass-shell, ℓ is always taken to mean either e or μ and q can be any of u, d, s, c or b.

⋆ e-mail: atlas.publications@cern.ch

[2]ATLAS uses a right-handed coordinate system with its origin at the nominal interaction point (IP) in the centre of the detector and the

con pixel detector, a silicon microstrip detector (SCT), and a transition radiation tracker (TRT). The ID is surrounded by a thin superconducting solenoid providing a 2 T magnetic field, and by high-granularity liquid-argon (LAr) sampling electromagnetic calorimeters. An iron-scintillator tile calorimeter provides hadronic coverage in the central rapidity range. The end-cap and forward regions are instrumented with LAr calorimetry for both electromagnetic and hadronic measurements. The muon spectrometer (MS) surrounds the calorimeters and consists of three large superconducting toroids, each with eight coils, a system of precision tracking chambers, and detectors for triggering.

The data used in this analysis were recorded in 2010 at the LHC at a centre-of-mass energy of 7 TeV. Application of beam, detector, and data-quality requirements results in a total integrated luminosity of 35 to 40 pb^{-1} depending on the search channel, with an estimated uncertainty of $\pm 3.4\%$ [17]. The events were triggered either by a single lepton or a pair of photon candidates with transverse momentum (p_T) thresholds which were significantly below the analysis offline requirements. The trigger introduces very little inefficiency except in one channel, $H \rightarrow WW \rightarrow \ell\nu qq$, where there are efficiency losses in the muon channel of about 16%.

Electron and photon candidates are reconstructed from energy clusters recorded in the liquid-argon electromagnetic calorimeter. The clusters must have shower profiles consistent with those expected from an electromagnetic shower. Electron candidates are matched to tracks reconstructed in the inner detector, while photon candidates require either no track or an identified conversion candidate. Muon candidates are reconstructed by matching tracks found in the inner detector with either tracks or hit segments in the muon spectrometer. Details of the quality criteria required on each of these objects differ amongst the analyses discussed here. There are in addition isolation criteria which again depend upon the specific backgrounds relevant to each analysis.

Jets are reconstructed from topological clusters [18] in the calorimeter using an anti-k_t algorithm [19] with a radius parameter $R = 0.4$. They are calibrated [18, 20] from the electromagnetic scale to the hadronic energy scale using p_T and η dependent correction factors based on Monte Carlo simulation and validated on data. They are required to have a p_T greater than 25 GeV unless otherwise stated. B tagging is performed using a secondary vertex algorithm based upon the decay length significance. A selection requirement is set to describe a jet as 'b-tagged' which has a 50% efficiency for true b-jets. The missing transverse energy is reconstructed

from topological energy clusters in the ATLAS calorimeters, with corrections for measured muons.

3 Cross sections, decays and simulation tools

3.1 Search for the standard model Higgs boson

At the LHC, the most important Standard Model Higgs boson production processes are the following four: gluon fusion ($gg \rightarrow H$), which couples to the Higgs boson via a heavy-quark triangular loop; fusion of vector bosons radiated off quarks ($qq \rightarrow qqH$); associated production with a vector boson ($q\bar{q} \rightarrow WH/ZH$); associated production with a top-quark pair ($q\bar{q}/gg \rightarrow t\bar{t}H$). The current calculations of the production cross sections have been gathered and summarised in Ref. [21].

Higher-order corrections have been calculated up to next-to-next-to-leading order (NNLO) in QCD for the gluon fusion [22–27], vector boson fusion [28] and associated WH/ZH production processes [29], and to next-to-leading order (NLO) for the associated production with a $t\bar{t}$ pair [30, 31]. In addition, QCD soft-gluon resummations up to next-to-next-to-leading log (NNLL) are available for the gluon fusion process [32]. The NLO electroweak (EW) corrections are applied to the gluon fusion [33, 34], vector boson fusion [35, 36] and the associated WH/ZH production [37] processes.

The Higgs boson decay branching ratios used take into account the recently calculated higher order QCD and EW corrections in each Higgs boson decay mode [21, 38]. The errors in these calculations for the states considered here are at most 2% and are neglected. For most four-fermion final states the predictions by Prophecy4f [39, 40] are used which include the complete NLO QCD+EW corrections with all interference and leading two-loop heavy Higgs boson corrections to the four-fermion width. The $H \rightarrow ZZ \rightarrow \ell\ell qq$ and $H \rightarrow ZZ \rightarrow \ell\ell\nu\nu$ analyses use the less precise single Z boson decay rates from Ref. [41].

The total signal production cross section in pp collisions at $\sqrt{s} = 7$ TeV, multiplied by the branching ratio for the final states considered in this paper, is summarised in Fig. 1 as a function of the Higgs boson mass. Sources of uncertainties on these cross sections include missing higher-order corrections, imprecise knowledge of the parton distribution functions (PDFs) and the uncertainty on the strong force coupling constant, α_s. These uncertainties are treated according to the recommendations given in Refs. [21, 42–45] and are $\pm(15$–$20)\%$ for the gluon fusion process, $\pm(3$–$9)\%$ for the vector boson fusion process and $\pm 5\%$ for the associated WH/ZH production process.

---

z-axis coinciding with the axis of the beam pipe. The x-axis points from the IP to the centre of the LHC ring, and the y-axis points upward. Cylindrical coordinates (r, ϕ) are used in the transverse plane, ϕ being the azimuthal angle around the beam pipe. The pseudorapidity is defined in terms of the polar angle θ as $\eta = -\ln\tan(\theta/2)$.
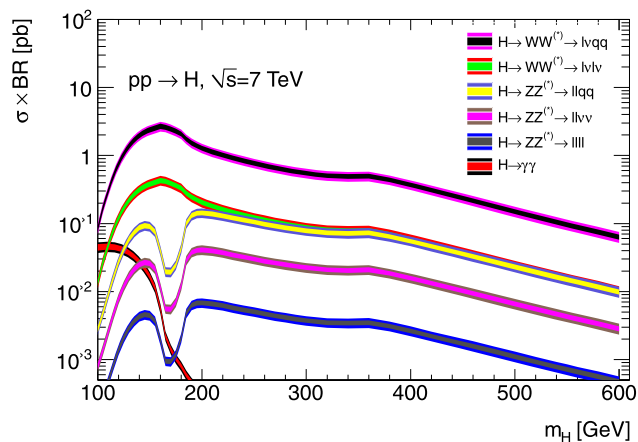
Fig. 1 The cross section multiplied by decay branching ratios for Standard Model Higgs boson production in pp collisions at a 7 TeV centre-of-mass energy as a function of mass [21]. All production modes are summed, and only final states considered in this paper are shown. Two bands are shown for each curve; the inner represents the QCD scale uncertainty and the outer also includes the α_s and PDF uncertainty

3.2 Higgs boson search in fourth generation models

Models with a fourth generation of heavy leptons and quarks with Standard Model-like couplings to the Higgs boson enhance its production cross section in gluon fusion by a factor of 4 to 10 compared to the predicted rate with three generations [46–49]. The model considered here [50] has very heavy fourth generation fermions, giving a minimum cross section but excluding the possibility that the Higgs boson decays to heavy neutrinos. These can weaken the exclusion for Higgs boson masses below the W pair threshold [51]. It should be noted that the branching ratio into photons is suppressed by a factor around 8 in this model.

The Higgs boson production cross section in the gluon fusion process and its decay branching ratios have been calculated in the fourth generation model at NLO with HIGLU [52] and HDECAY [38]. The NNLO+NNLL QCD corrections are applied to the gluon fusion cross sections. The QCD corrections for the fourth generational model are assumed to be the same as in the Standard Model. The full two-loop Standard Model electroweak corrections [33, 34] are taken into account. The effect of a fourth generation in the Standard Model background processes, which includes contributions from loop diagrams, has been neglected.

3.3 Monte Carlo simulations

For the $H \rightarrow ZZ$ Monte Carlo samples, the Higgs signal is generated using PYTHIA [53] interfaced to PHOTOS [54] for final-state radiation. The $H \rightarrow WW^{(*)} \rightarrow \ell\nu\ell\nu$ events produced by gluon fusion or vector boson fusion are modelled using the MC@NLO [55, 56] and SHERPA [57]

Monte Carlo generators, respectively. $H \rightarrow WW \rightarrow \ell\nu qq$ is modelled using PYTHIA for the gluon fusion and HERWIG [58] for vector boson fusion. The $\gamma\gamma$ signal is simulated with MC@NLO, HERWIG and PYTHIA for the gluon fusion, vector boson fusion and associated production processes respectively.

For background sample generation, the PYTHIA, ALPGEN [59], MC@NLO, MADGRAPH [60], SHERPA and HERWIG packages are employed.

All Monte Carlo samples are processed through a complete simulation of the ATLAS detector [61] using the GEANT programme [62].

4 Search for $H \rightarrow \gamma\gamma$

The search for the Higgs boson in the $\gamma\gamma$ decay mode is described below; further details can be found in Ref. [7]. The event selection requires the presence of at least two identified photons [63], including converted photons, isolated from any other activity in the calorimeter. The leading and the sub-leading photons are required to have transverse momenta above 40 GeV and 25 GeV, respectively. The directions of the photons are measured using the position determined in the first sampling of the electromagnetic calorimeter and that of the reconstructed primary vertex. The di-photon invariant mass spectrum is used to search for a peak above the background contributions.

The main background processes in the $H \rightarrow \gamma\gamma$ search arise from the production of two isolated prompt photons ($\gamma\gamma$) and from fake photons in photon-jet (γj) and di-jet (jj) events. Fake photons can originate from jets in which a leading π^0 or η meson from the quark or gluon fragmentation is reconstructed as a single isolated photon. Each of these background contributions has been estimated from sideband control samples in the data. The background from Drell–Yan events, $Z/\gamma^* \rightarrow ee$, where the electrons are mistakenly identified as photons, is estimated from studies of the Z boson mass peak and extrapolated to the signal region. The total number of estimated background events is constrained to be the observed number. The di-photon invariant mass distribution for the events passing the full selection is shown in Fig. 2. The full-width at half maximum of a signal with $m_h = 120$ GeV would be 4.2 GeV.

The expected signal yield, summing all production processes, and estimated background composition for a total integrated luminosity of 38 pb^{-1} are summarised in Table 1. A total of 99 events passing all selection criteria are observed in data in the di-photon mass range from 100 GeV to 150 GeV. The background in this region is modelled by fitting an exponential function to the data. The signal peak is modelled by a Gaussian core portion and a power-law low-end tail [64]. Tails in the signal resolution are modelled
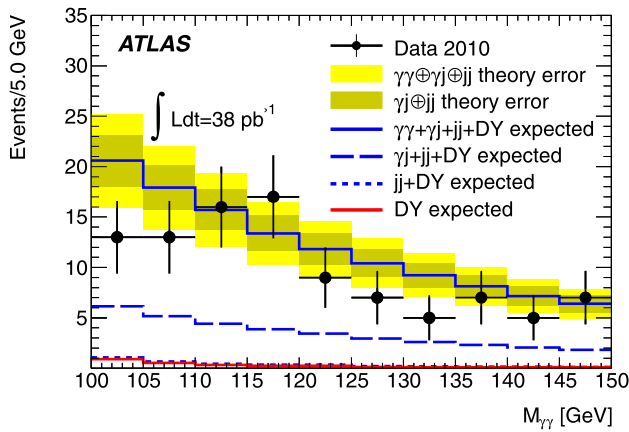
Fig. 2 Distribution of the di-photon invariant mass for the 99 events from data passing all event selection criteria in the $H \rightarrow \gamma\gamma$ search and for the Monte Carlo prediction. The overall uncertainty on the expected total yield is illustrated by the *yellow band*. The uncertainty due to the reducible background is also shown (*dark yellow band*). The predictions for the main components of the background (di-photon, photon-jet, jet-jet and Drell-Yan) are also illustrated

Table 1 The number of expected and observed events in the $H \rightarrow \gamma\gamma$ search in the di-photon mass range from 100 GeV to 150 GeV for an integrated luminosity of 38 pb^{-1}. Also shown is the composition of the background expected from Monte Carlo simulation and the division of the observed data as discussed in the text as well as the expected number of $H \rightarrow \gamma\gamma$ signal events for a Higgs boson mass of $m_H = 120$ GeV. Total uncertainties are shown in the middle column while in the rightmost column the statistical and systematic uncertainties, respectively, are given

Total	Expected	Observed or Estimated
	120 ± 27	99
$\gamma\gamma$	86 ± 23	$75.0 \pm 13.3^{+2.7}_{-3.6}$
γj	31 ± 15	$19.6 \pm 7.5 \pm 3.9$
jj	1 ± 1	$1.5 \pm 0.7^{+1.8}_{-0.5}$
Z/γ^*	2.7 ± 0.2	$2.9 \pm 0.1 \pm 0.6$
$H \rightarrow \gamma\gamma$	$0.45^{+0.11}_{-0.10}$	($m_H = 120$ GeV)

by a wide Gaussian component of small amplitude. No significant excess of events over the continuous background is found for any Higgs boson mass. The systematic uncertainty on the total signal acceptance is $\pm 15\%$, where the dominant contributions come from photon identification ($\pm 11\%$) and photon isolation efficiencies ($\pm 10\%$).

5 Search for $H \rightarrow WW$

The search for the Higgs boson in the decay channel $H \rightarrow WW$ benefits from the large branching ratio of the Higgs boson to decay into a pair of W bosons for masses above $m_H \gtrsim 110$ GeV, the sizable W boson decay rates to leptons and the powerful identification of leptons with

the ATLAS detector. It offers the greatest sensitivity of any search channel when the Higgs boson mass is close to twice the W boson mass, $m_H \sim 165$ GeV. Two different decay modes of the W bosons are considered: the $H \rightarrow WW^{(*)} \rightarrow \ell\nu\ell\nu$ channel is pursued for Higgs boson masses in the range from 120 GeV to 200 GeV, and the $H \rightarrow WW \rightarrow \ell\nu qq$ decay mode is used for Higgs boson masses in the range from 220 GeV to 600 GeV. The analyses are described below and further details can be found in Refs. [8, 9].

5.1 Search for $H \rightarrow WW^{(*)} \rightarrow \ell\nu\ell\nu$

The $H \rightarrow WW^{(*)} \rightarrow \ell\nu\ell\nu$ analysis is performed using a dataset corresponding to an integrated luminosity of 35 pb^{-1}. Events are selected requiring exactly two isolated leptons with opposite charge. The leading lepton is required to have $p_T > 20$ GeV and the sub-leading lepton is required to have $p_T > 15$ GeV. Events are classified into three channels depending on the lepton flavours: $e\mu$, ee or $\mu\mu$. If the two leptons are of the same flavour, their invariant mass ($m_{\ell\ell}$) is required to be above 15 GeV to suppress background from Υ production. To increase the sensitivity, the selections are then allowed to depend on the Higgs boson mass hypothesis. For all lepton combinations in the low (high) mass Higgs boson search, $m_{\ell\ell}$ is required to be below 50 (65) GeV for Higgs boson masses $m_H \leq 170$ GeV ($m_H > 170$ GeV) which suppress backgrounds from top-quark production and Z boson production. The missing transverse energy in the event is required to be $E_T^{miss} > 30$ GeV. An upper bound is imposed on the azimuthal angle between the two leptons, $\Delta\phi_{\ell\ell} < 1.3$ (1.8) radians, taking advantage of the spin correlations [65] expected in the Higgs boson decay. The signal region is defined by the transverse mass (m_T) [66]:

$$m_T = \sqrt{\left(E_T^{\ell\ell} + E_T^{miss}\right)^2 - \left(\mathbf{P}_T^{\ell\ell} + \mathbf{P}_T^{miss}\right)^2}, \quad (1)$$

where $E_T^{\ell\ell} = \sqrt{(\mathbf{P}_T^{\ell\ell})^2 + m_{\ell\ell}^2}$, $|\mathbf{P}_T^{miss}| = E_T^{miss}$ and $\mathbf{P}_T^{\ell\ell}$ is the transverse momentum of the dilepton system. The transverse mass is required to be $0.75 \cdot m_H < m_T < m_H$ for the event to be considered in a given m_H range. Events are also treated separately depending on whether they have zero jets (0-jet channel) or one jet (1-jet channel) reconstructed with $|\eta| < 4.5$ due to the differences in background composition and expected signal-to-background ratio. To suppress background from top-quark production, events in the 1-jet channel are rejected if the jet is identified as coming from a b-quark. Events with two or more jets have been analysed as a separate channel. However, due to the marginal contribution to the overall sensitivity given the current total integrated luminosity and the additional systematic uncertainties, this channel is not included in this combination.

The expected background contributions from WW, top-quark and $W+$jets production are normalised using dedicated control regions in data as described in the next sections. Other smaller backgrounds are normalised according to their theoretical cross sections. The background from $Z/\gamma^* +$jets production is normalised to the theoretical cross section with a correction factor determined from data.

5.1.1 The WW background

The di-boson WW continuum can be distinguished from the Higgs boson signal through the kinematic selections. A control region is defined by changing the cut on $m_{\ell\ell}$ to require over 80 GeV (but not within 10 GeV of the Z boson mass if the leptons are of the same flavour) and removing the selections on m_T and $\Delta\phi_{\ell\ell}$. The expected ratio of the background contribution in the control region and in the signal region is taken from Monte Carlo simulation. The three main sources of systematic uncertainty affecting this ratio are the theoretical uncertainty on the extrapolation, the jet energy scale uncertainty and the limited statistics in the simulated sample. Uncertainties due to these effects of $\pm6\%$ in the 0-jet channel and $\pm17\%$ in the 1-jet channel have been determined.

5.1.2 The $t\bar{t}$ and single top-quark backgrounds

Top-quarks, whether from strong interaction $t\bar{t}$ production or weak interaction single top-quark production, are a copious source of final states with one or two W bosons accompanied by one or more jets. Due to kinematic selection one or more of these jets may fail identification, thereby leading to a final state similar to that from the $H \to WW$ signal.

The background from top-quark production in the 0-jet channel is estimated by first removing the jet veto. This gives a sample dominated by top-quarks, and the expected contamination from other processes in the control region is subtracted from the observed event yield. Then the probability that top events pass the jet veto is derived from the measured probability of not reconstructing a jet in data, using a sample of top candidates with two leptons, one b-jet and no other jet. The dominant systematic uncertainties originate from the limited statistics in data and the jet energy scale. A total uncertainty of $\pm60\%$ has been determined for the top-quark background estimate in the 0-jet channel.

The top-quark background in the 1-jet channel is normalised using a control region where the veto on jets coming from b-quarks is reversed and the $\Delta\phi_{\ell\ell}$, $m_{\ell\ell}$ and m_T selections are removed. An extrapolation factor from the control region to the signal region is estimated from Monte Carlo simulation. The dominant systematic uncertainties on the top-quark background estimate in the 1-jet channel are $\pm23\%$ from the theoretical uncertainties on the extrapolation factor and $\pm22\%$ from the uncertainty on the b-tagging efficiency.

5.1.3 The $W+$jets background

The production of W bosons accompanied by jets can mimic the $H \to WW$ signal if one of the jets is mis-identified as an isolated lepton. The $W+$jets background is normalised using a control region defined by relaxing the identification and isolation criteria for one of the two leptons. The contribution to the signal region is estimated by multiplying the rate measured in the control region by the probability for fake leptons which pass the relaxed identification and isolation criteria to also pass the original lepton selection criteria. This misidentification probability is measured in a multi-jet data sample. The major sources of systematic uncertainty for the $W+$jets background estimate come from the bias introduced by the jet trigger threshold used to select the multi-jet events and the residual difference in kinematics and flavour composition of the jets in multi-jet events and in events from $W+$jets production. The total uncertainty on the estimated $W+$jets background is $\pm50\%$.

5.1.4 The $Z/\gamma^* +$jets background

The largest cross section for producing two isolated, high-p_T leptons comes from the $Z/\gamma^* \to \ell\ell$ process. The background from $Z/\gamma^* +$jets is significantly reduced by the upper bound on $m_{\ell\ell}$ and the requirement of high E_T^{miss} in the signal region. To correct for potential mis-modelling of the distribution of E_T^{miss} at high values, a correction factor is derived from the observed difference between the fraction of events passing the $E_T^{miss} > 30$ GeV selection in data and Monte Carlo simulation for events with $m_{\ell\ell}$ within 10 GeV of the Z boson mass [41]. As the discrepancy between data and Monte Carlo tends to be larger in events with jets, the correction factor is larger in the 1-jet channel than in the 0-jet channel. The flavours of the two leptons in the event also impact the magnitude of the correction factor, since any discrepancies between data and simulation have different sources. In the 1-jet channel, the correction factors are found to be $1.2 \pm 0.4 \pm 0.1$[3] in the ee analysis and $2.4 \pm 0.5 \pm 0.2$ in the $\mu\mu$ analysis. Under the assumption that the same correction factors apply to events below the upper bound on $m_{\ell\ell}$, the expected $Z/\gamma^* +$jets background is obtained from the Monte Carlo simulation normalised to the product of the theoretical cross section and the correction factors.

5.1.5 Results for the $H \to WW^{(*)} \to \ell\nu\ell\nu$ search

The expected and observed numbers of events in the $H \to WW$ analysis for a Higgs boson mass of 170 GeV are shown in Table 2. Three events in total are observed in the 0-jet

---

[3] When two errors are quoted the first is statistical and the second systematic.

Table 2 Numbers of expected signal ($m_H = 170$ GeV) and background events and the observed numbers of events in the data passing all selections in the $H \to WW^{(*)} \to \ell\nu\ell\nu$ search. The dataset used in this analysis corresponds to an integrated luminosity of 35 pb^{-1}. The uncertainties shown are the statistical and systematic uncertainties respectively

	$e\mu$	ee	$\mu\mu$
0-jet channel			
WW	$0.71 \pm 0.05 \pm 0.06$	$0.20 \pm 0.03 \pm 0.02$	$0.53 \pm 0.02 \pm 0.05$
$t\bar{t}$ and single top	$0.09 \pm 0.05 \pm 0.06$	$0.03 \pm 0.01 \pm 0.02$	$0.08 \pm 0.04 \pm 0.06$
$WZ/ZZ/W\gamma$	$0.020 \pm 0.001 \pm 0.001$	$0\,(<0.001) \pm 0$	$0.010 \pm 0.001 \pm 0.001$
$Z/\gamma^* + \mathrm{jets}$	$0\,(<0.001) \pm 0$	$0\,(<0.001) \pm 0$	$0\,(<0.002) \pm 0$
$W + \mathrm{jets}$	$0.01 \pm 0.01 \pm 0.01$	$0.02 \pm 0.01 \pm 0.01$	$0 \pm 0.10 \pm 0.01$
Total Background	$0.83 \pm 0.07 \pm 0.13$	$0.25 \pm 0.08 \pm 0.04$	$0.62 \pm 0.05 \pm 0.10$
$H \to WW^{(*)} \to \ell\nu\ell\nu$	$0.62 \pm 0.01 \pm 0.18$	$0.20 \pm 0.01 \pm 0.07$	$0.44 \pm 0.01 \pm 0.12$
Observed	1	1	1
1-jet channel			
WW	$0.18 \pm 0.03 \pm 0.03$	$0.05 \pm 0.02 \pm 0.01$	$0.16 \pm 0.03 \pm 0.02$
$t\bar{t}$ and single top	$0.26 \pm 0.07 \pm 0.11$	$0.10 \pm 0.02 \pm 0.04$	$0.15 \pm 0.04 \pm 0.07$
$WZ/ZZ/W\gamma$	$0.01 \pm 0.001 \pm 0.001$	$0\,(<0.001) \pm 0$	$0\,(<0.001) \pm 0$
$Z/\gamma^* + \mathrm{jets}$	$0\,(<0.01) \pm 0$	$0.05 \pm 0.02 \pm 0.02$	$0.25 \pm 0.08 \pm 0.05$
$W + \mathrm{jets}$	$0.02 \pm 0.02 \pm 0.01$	$0.03 \pm 0.20 \pm 0.01$	$0 \pm 0.10 \pm 0.01$
Total Background	$0.47 \pm 0.08 \pm 0.16$	$0.23 \pm 0.04 \pm 0.06$	$0.56 \pm 0.09 \pm 0.14$
$H \to WW^{(*)} \to \ell\nu\ell\nu$	$0.31 \pm 0.01 \pm 0.09$	$0.08 \pm 0.01 \pm 0.03$	$0.21 \pm 0.01 \pm 0.06$
Observed	0	0	1

channel for the combined ee, $e\mu$ and $\mu\mu$ final states, compared to an expected number of events from background sources only of $1.70 \pm 0.12 \pm 0.17$. More events are expected in the $\mu\mu$ channel compared to the ee channel due to different lepton identification efficiencies for electrons and muons. In the 1-jet channel, one event is observed in the data compared to a total number of expected events from background sources of $1.26 \pm 0.13 \pm 0.23$. The observed m_T distributions in data after all selections except the transverse mass cut for the combined $e\mu$, ee and $\mu\mu$ channels are compared to the expected distributions from simulated events in Fig. 3.

5.2 Search for $H \to WW \to \ell\nu qq$

The $H \to WW \to \ell\nu qq$ analysis uses a dataset corresponding to an integrated luminosity of 35 pb^{-1}. Events are selected requiring exactly one lepton with $p_T > 30$ GeV. The missing transverse energy in the event is required to be $E_T^{\mathrm{miss}} > 30$ GeV. Events with fewer than two jets are rejected.[4] Events with ≥ 4 jets are treated as a separate search channel, which is however not included in the current combination. The pair of jets with invariant mass closest to the W boson mass is considered to be coming from the W boson and the measured mass must be between 71 GeV and

91 GeV. The event is rejected if any of the jets in the event is identified as coming from a b-quark. The invariant mass of the Higgs boson candidate, $m_{\ell\nu qq}$, is reconstructed with a W boson mass constraint on the lepton-neutrino system giving rise to a quadratic equation. If there are two solutions the one corresponding to the lower longitudinal momentum is taken; if complex the real part is used.

The dominant source of background events in the $H \to WW \to \ell\nu qq$ search comes from $W + \mathrm{jets}$ production. The contribution from QCD events is estimated by fitting the observed E_T^{miss} distribution as the sum of templates taken from simulation. Table 3 shows the expected numbers of signal and background events in the signal region, as well as the observation. In the channel with only two and no additional jets, 450 events are observed in the data passing all selection criteria compared to an expected yield from background sources of 450 ± 41 events. In the channel with one extra jet 263 events are observed, compared to an expected number of background events of 224 ± 15.

The distributions of the invariant mass for the Higgs boson candidates in data are compared to the expected distributions from simulated events in Fig. 4. The $m_{\ell\nu qq}$ background spectrum is modelled with a falling exponential function. The impact of the functional form has been investigated by replacing the single exponential with a double exponential, by histograms taken from simulation, and by a mixture of both methods without significant change in the results. It should be noted that the limit extraction is made using the

---

[4]In this channel the jet p_T threshold is raised from 25 GeV to 30 GeV.

exponential fit, not by comparison with the simulated background.
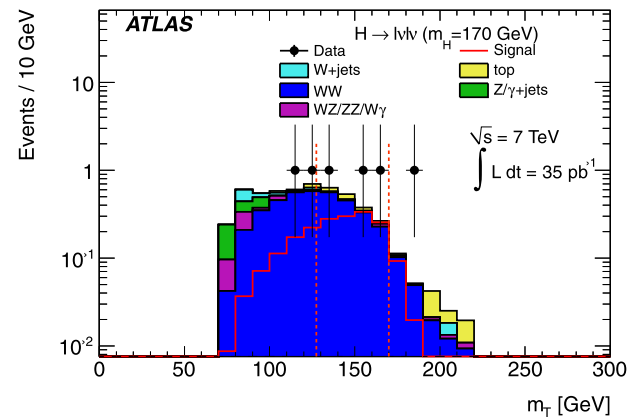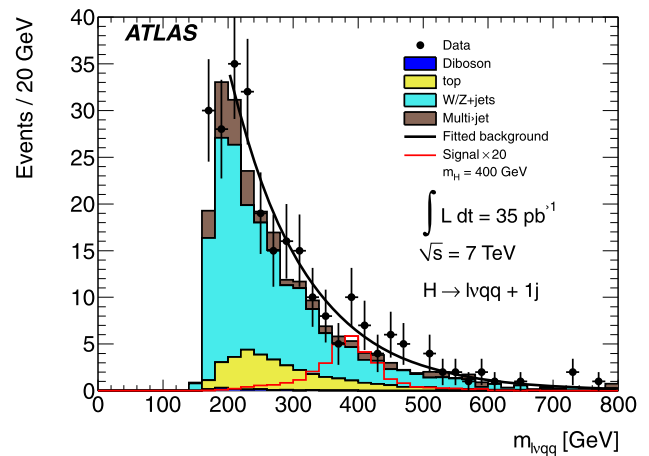

(a) 0-jet channel
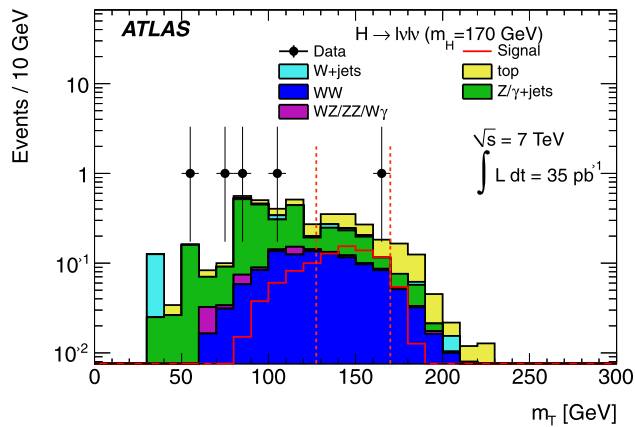
(b) 1-jet channel

Fig. 3 Distributions of the transverse mass m_T in the 0-jet channel (**a**) and 1-jet channel (**b**) for the $H \rightarrow WW^{(*)} \rightarrow \ell\nu\ell\nu$ search after all selections except the transverse mass cut for the combined $e\mu$, ee and $\mu\mu$ channels. The error bars reflect Poisson asymmetric errors. A Higgs boson signal is shown for $m_H = 170$ GeV. The selections applied for $m_H = 170$ GeV are indicated by the two *vertical dotted lines*
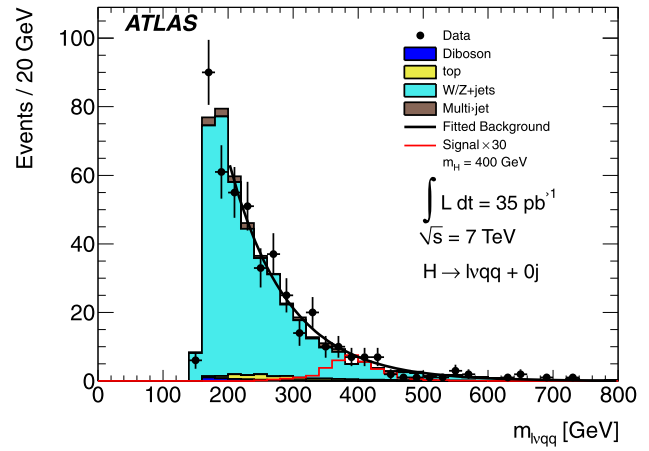
(a) 0 extra jet channel

(b) 1 extra jet channel

Fig. 4 Distributions of the invariant mass $m_{\ell\nu qq}$ for the $H \rightarrow WW \rightarrow \ell\nu qq$ search after the application of all selection criteria and the W-mass constrained fit. The background fit is shown as a *continuous line*. In (**a**) no extra jets are allowed and in (**b**) one additional jet is required. The Higgs boson signal is shown for $m_H = 400$ GeV and the expected yield is scaled up by a factor of 30 for illustration purposes

Table 3 Numbers of expected signal ($m_H = 400$ GeV) and background events and the observed numbers of events in the data passing all selections in the $H \rightarrow WW \rightarrow \ell\nu qq$ search. The dataset used corresponds to an integrated luminosity of 35 pb^{-1}. The quoted uncertainties are combinations of the statistical and systematic uncertainties

$m_H = 400$ GeV	$H + 0$-jets		$H + 1$-jet	
	$e\nu qq$	$\mu\nu qq$	$e\nu qq$	$\mu\nu qq$
$W/Z + $jets	157 ± 22	259 ± 34	39.1 ± 6.2	119 ± 12
Multi-jet	11.1 ± 1.6	4.5 ± 0.6	17.7 ± 2.8	13.3 ± 1.3
Top	5.3 ± 1.7	7.7 ± 2.5	15.5 ± 5.0	18.2 ± 5.8
Di-boson	1.8 ± 0.3	3.0 ± 0.4	0.6 ± 0.1	0.9 ± 0.1
Total Background	175 ± 22	275 ± 34	72.9 ± 8.4	151 ± 13
$H \rightarrow WW \rightarrow \ell\nu qq$	0.5 ± 0.2	0.6 ± 0.2	0.5 ± 0.2	0.5 ± 0.2
Observed	177	273	87	176

6 Search for $H \to ZZ^{(*)}$

Three different $H \to ZZ^{(*)}$ final states are considered here: $H \to ZZ^{(*)} \to \ell\ell\ell\ell$, $H \to ZZ \to \ell\ell\nu\nu$ and $H \to ZZ \to \ell\ell qq$. In the $H \to ZZ^{(*)} \to \ell\ell\ell\ell$ search, the excellent energy and momentum resolutions of the ATLAS detector for electrons and muons lead to a narrow expected four-lepton invariant mass peak on top of a continuous background. The dominant background component is the irreducible $ZZ^{(*)} \to \ell\ell\ell\ell$ process. In the low Higgs boson mass region, where one of the Z bosons is off-shell and decays into a pair of low transverse momentum leptons, the reducible backgrounds from Z + jets production and $t\bar{t}$ production are also important. For Higgs boson masses above $m_H \gtrsim 200$ GeV both Z bosons are on-shell. In this region the decay modes $H \to ZZ \to \ell\ell qq$ and $H \to ZZ \to \ell\ell\nu\nu$, which have substantially larger branching ratios but also larger backgrounds compared to the $H \to ZZ^{(*)} \to \ell\ell\ell\ell$ decay, provide additional sensitivity. The analyses of the $H \to ZZ \to \ell\ell qq$ and $H \to ZZ \to \ell\ell\nu\nu$ channels require that both Z bosons are on-shell, which limits the contribution from the reducible backgrounds from Z + jets production and $t\bar{t}$ production. In this paper the $H \to ZZ \to \ell\ell qq$ and $H \to ZZ \to \ell\ell\nu\nu$ search channels have been used for Higgs boson masses in the range $200\,\text{GeV} \le m_H \le 600\,\text{GeV}$, a range extending beyond the sensitivities of LEP and Tevatron experiments [4, 6]. Further details of the three analyses can be found in Refs. [10, 11].

6.1 Search for $H \to ZZ^{(*)} \to \ell\ell\ell\ell$

Candidate events are selected requiring two same-flavour and opposite-charge pairs of leptons. Muons with $p_T > 7$ GeV and electrons with $p_T > 15$ GeV are considered, while at least two out of the four leptons must satisfy $p_T > 20$ GeV. All leptons are required to be well separated from each other, isolated from other activity in the tracking detectors and the calorimeters and have low track impact parameters with respect to the primary vertex. At least one of the lepton pairs is required to have an invariant mass within 15 GeV (within 12 GeV if the combined four-lepton mass is high) of the Z boson mass. The requirement on the invariant mass of the second lepton pair varies as a function of the Higgs boson candidate mass, $m_{\ell\ell\ell\ell}$. The effective Higgs boson candidate mass resolution $\sigma(m_H)$, including the intrinsic width at the Higgs boson mass hypothesis being tested, is used to define an allowed range for the reconstructed Higgs boson candidate mass. The latter is required to be within $\pm 5\sigma(m_H)$ of the tested Higgs boson mass for the event to be considered.

The magnitude of the $ZZ^{(*)}$ background is normalised to the measured Z boson cross section multiplied by the expected ratio of the cross sections σ_{ZZ}/σ_Z from theoretical calculations [67]. This estimate is independent of the luminosity uncertainty, and the cross section ratio is less affected by theoretical uncertainties than the σ_{ZZ} cross section alone. The total uncertainty on the $ZZ^{(*)}$ background estimate is $\pm 15\%$. The reducible Z + jets background arises predominantly from Z boson production in association with a pair of heavy flavour quarks which decay semi-leptonically. This background is normalised using dedicated control regions in data where the lepton identification requirements are relaxed for the second pair of leptons. The final uncertainty on the Z + jets background is $\pm 20\%$. The $t\bar{t}$ background is estimated from Monte Carlo simulation and normalised to its theoretical cross section. A total uncertainty of $\pm 25\%$ is estimated for the $t\bar{t}$ background contribution.

After the application of all selection criteria, no candidate events remain in data for the $H \to ZZ^{(*)} \to \ell\ell\ell\ell$ search at any Higgs boson mass. This is consistent with the small background and signal yields expected with the integrated luminosity of 40 pb^{-1} used in this analysis. The results are shown in Table 4 for two selected Higgs boson masses of $m_H = 130$ GeV and $m_H = 200$ GeV. The distribution of the Higgs boson candidate invariant mass, $m_{\ell\ell\ell\ell}$, before applying the lepton impact parameter and isolation requirements is shown in Fig. 5.

Table 4 Expected signal and background event yields in the $H \to ZZ^{(*)} \to \ell\ell\ell\ell$ search within $\pm 5\sigma(m_H)$ for two selected Higgs boson masses. No events are observed in the data. The dataset used corresponds to a total integrated luminosity of 40 pb^{-1}. The quoted uncertainties are combinations of the statistical and systematic uncertainties

m_H (GeV)	130	200
Total background	0.010 ± 0.002	0.090 ± 0.014
$H \to ZZ^{(*)} \to \ell\ell\ell\ell$	0.015 ± 0.003	0.095 ± 0.017
Observed	0	0

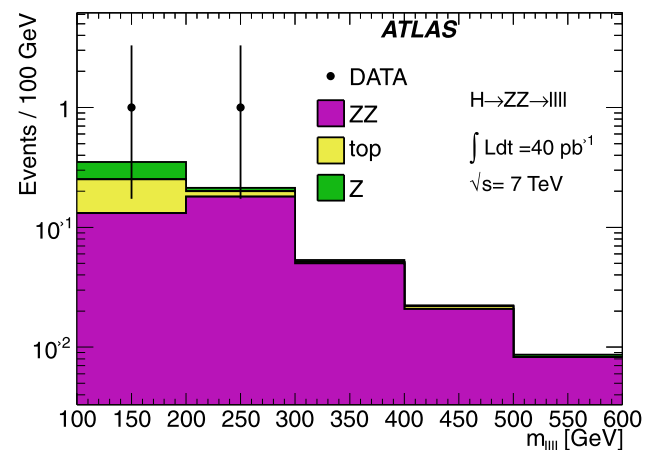**Fig. 5** Distribution of $m_{\ell\ell\ell\ell}$ in the $H \to ZZ^{(*)} \to \ell\ell\ell\ell$ search before applying the lepton impact parameter and isolation requirements which remove the two candidates. The error bars reflect Poisson asymmetric errors

6.2 Search for $H \rightarrow ZZ \rightarrow \ell\ell qq$

Events are selected requiring exactly two same-flavour leptons with an invariant mass 76 GeV $< m_{\ell\ell} <$ 106 GeV and at least two jets. To reduce background from top production the missing transverse energy is required to be $E_T^{miss} <$ 50 GeV. The two jets in the event with the highest individual p_T are required to have an invariant mass, m_{jj}, in the range 70 GeV $< m_{jj} <$ 105 GeV. Additional background rejection is obtained for high mass by using the fact that the final state jets and leptons are boosted in the directions of the two Z bosons. For Higgs boson searches at $m_H \geq$ 360 GeV, the two jets are required to have $p_T >$ 50 GeV. Furthermore, the azimuthal angles between the two jets, $\Delta\phi_{jj}$, and between the two leptons, $\Delta\phi_{\ell\ell}$, must both be less than $\pi/2$.

The Higgs boson candidate mass is constructed from the invariant mass of the two leptons and the two jets in the event, $m_{\ell\ell jj}$. The two jets are constrained to have an invariant mass equal to the Z boson mass to improve the Higgs boson candidate mass resolution.

6.2.1 Background estimates for the $H \rightarrow ZZ \rightarrow \ell\ell qq$ search

The dominant background in the $H \rightarrow ZZ \rightarrow \ell\ell qq$ search channel is expected to come from $Z +$ jets production. Other significant sources are $t\bar{t}$ production, multi-jet production and ZZ/WZ production. All backgrounds, except for the multi-jet background, are estimated from Monte Carlo simulation. For the $Z +$ jets and the $t\bar{t}$ backgrounds the predictions from simulation are compared against data in control samples which are dominated by these backgrounds. The $Z +$ jets control region is defined by modifying the m_{jj} selection to instead require 40 GeV $< m_{jj} <$ 70 GeV or 105 GeV $< m_{jj} <$ 150 GeV. The $t\bar{t}$ control region is defined by reversing the E_T^{miss} selection and modifying the $m_{\ell\ell}$ selection to require 60 GeV $< m_{\ell\ell} <$ 76 GeV or 106 GeV $< m_{\ell\ell} <$ 150 GeV. Both the $Z +$ jets and the $t\bar{t}$ background estimates from Monte Carlo simulation are found to be in

good agreement with data in the control samples. The contribution from $W +$ jets is very small and assumed to be adequately modelled. The multi-jet background in the electron channel is derived from a sample where the electron identification requirements are relaxed. In the muon channel, the multi-jet background is taken from Monte Carlo after verifying the accuracy of the simulation using a data sample where the two muons in the event are required to have the same charge.

6.2.2 Results for the $H \rightarrow ZZ \rightarrow \ell\ell qq$ search

The $H \rightarrow ZZ \rightarrow \ell\ell qq$ analysis is performed for Higgs boson masses between 200 GeV and 600 GeV in steps of 20 GeV. Table 5 summarises the numbers of estimated background events and observed events in data for the selections below and above $m_H =$ 360 GeV. The numbers of expected signal events for two representative Higgs boson masses are also shown. For the low mass search, 216 events are observed in data passing all selection criteria compared to an expected number of events from background sources only of $226 \pm 4 \pm 28$ events. The corresponding numbers for the high mass searches are 11 events observed in data compared to an expected yield of $9.9 \pm 0.9 \pm 1.5$ events from background sources only. The distribution of the reconstructed Higgs boson candidate mass $m_{\ell\ell jj}$ for the events passing all of the selection criteria is shown in Fig. 6.

6.3 Search for $H \rightarrow ZZ \rightarrow \ell\ell\nu\nu$

The $H \rightarrow ZZ \rightarrow \ell\ell\nu\nu$ final state is characterised by two charged leptons and large E_T^{miss}. Events are selected by requiring exactly two leptons of the same flavour with an invariant mass 76 GeV $< m_{\ell\ell} <$ 106 GeV. Events are rejected if any jet is identified as coming from a b-quark. The selection has been optimised separately for searches at low ($m_H <$ 280 GeV) and high ($m_H \geq$ 280 GeV) values of the Higgs boson mass. Events are required to have $E_T^{miss} >$ 66 (82) GeV and $\Delta\phi_{\ell\ell} <$ 2.64 (2.25) radians for

Table 5 Numbers of events estimated as background, observed in data and expected from signal in the $H \rightarrow ZZ \rightarrow \ell\ell qq$ search for low mass ($m_H <$ 360 GeV) and high mass ($m_H \geq$ 360 GeV) selections. The signal, quoted at two mass points, includes small contributions from $\ell\ell\ell\ell$ and $\ell\ell\nu\nu$ decays. Electron and muon channels are combined. The uncertainties shown are the statistical and systematic uncertainties, respectively

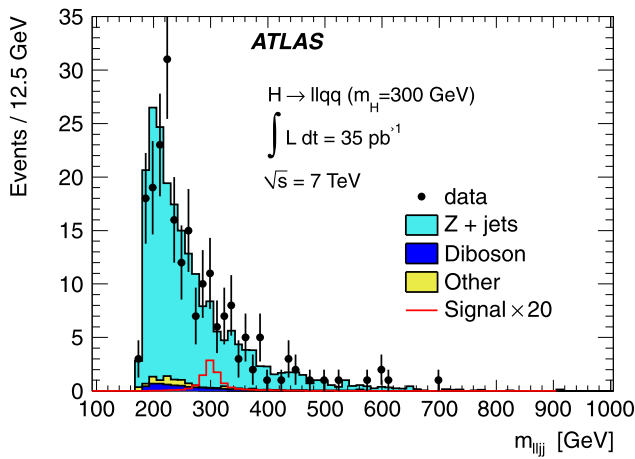| Source	Low mass selection	High mass selection
$Z +$ jets	$214 \pm 4 \pm 27$	$9.1 \pm 0.9 \pm 1.4$
$W +$ jets	$0.33 \pm 0.16 \pm 0.17$	–
$t\bar{t}$	$0.94 \pm 0.09 \pm 0.25$	$0.08 \pm 0.02 \pm 0.03$
Multi-jet	$3.81 \pm 0.65 \pm 1.91$	$0.11 \pm 0.11 \pm 0.06$
ZZ	$3.80 \pm 0.10 \pm 0.73$	$0.30 \pm 0.03 \pm 0.06$
WZ	$2.83 \pm 0.05 \pm 0.88$	$0.29 \pm 0.02 \pm 0.10$
Total background	$226 \pm 4 \pm 28$	$9.9 \pm 0.9 \pm 1.5$
$H \rightarrow ZZ \rightarrow \ell\ell qq$	$0.60 \pm 0.01 \pm 0.12$ ($m_H =$ 200 GeV)	$0.24 \pm (< 0.001) \pm 0.05$ ($m_H =$ 400 GeV)
Observed	216	11

Fig. 6 Distribution of $m_{\ell\ell jj}$ for events passing all of the selection criteria in the $H \to ZZ \to \ell\ell qq$ search. The expected yield for a Higgs boson with a mass $m_H = 300$ GeV is also shown, multiplied by a factor of 20 for illustrative purposes. The contribution labelled "Other" is mostly from top events but includes also QCD multijet production

the low (high) mass region. For the low mass region $\Delta\phi_{\ell\ell} > 1$ radian is also required. The Higgs boson candidate transverse mass is obtained from the invariant mass of the two leptons and the missing transverse energy.

6.3.1 Background estimates for the $H \to ZZ \to \ell\ell\nu\nu$ search

A major background in the $H \to ZZ \to \ell\ell\nu\nu$ search channel comes from di-boson production and is estimated from Monte Carlo simulation. Background contributions from $t\bar{t}$ and W + jets production are also obtained from Monte Carlo simulation, and the estimated yields are verified by comparing with the number of observed events in dedicated control samples in the data. Both the $t\bar{t}$ and the W + jets con-

trol regions are defined by modifying the $m_{\ell\ell}$ selection to instead require 60 GeV $< m_{\ell\ell} < 76$ GeV or 106 GeV $< m_{\ell\ell} < 150$ GeV. The $t\bar{t}$ control region also requires that the events pass $E_T^{miss} > 20$ GeV and that at least one jet is identified as coming from a b-quark. The W + jets control region instead requires $E_T^{miss} > 36$ GeV and that no jets in the events are identified as coming from a b-quark. The observed event yields in the control regions for $t\bar{t}$ and W + jets production are in good agreement with the predictions from the Monte Carlo simulation. The background from Z + jets production is estimated from Monte Carlo simulation after comparison studies of the E_T^{miss} distribution between Monte Carlo and data. The multi-jet background in the electron channel is derived from a sample where the electron identification requirements are relaxed. In the muon channel, the multi-jet background is estimated from a simulated sample of semi-leptonically decaying b- and c-quarks and found to be negligible after the application of the $m_{\ell\ell}$ selection. This was verified in data using leptons with identical charges.

6.3.2 Results for the $H \to ZZ \to \ell\ell\nu\nu$ search

The $H \to ZZ \to \ell\ell\nu\nu$ analysis is performed for Higgs boson masses between 200 GeV and 600 GeV in steps of 20 GeV. Table 6 summarises the numbers of events observed in the data, the estimated numbers of background events and the expected numbers of signal events for two selected m_H values. For the low mass selections, five events are observed in data compared to an expected number of events from background sources only of $5.8 \pm 0.5 \pm 1.3$. The corresponding results for the high mass selections are five events observed in data compared to an expected yield of $3.5 \pm 0.4 \pm 0.8$ events from background sources only. In addition to the $H \to ZZ \to \ell\ell\nu\nu$ decays, several other Higgs boson channels give a non-negligible contribution to

Table 6 Numbers of events estimated from background, observed in data and expected from signal in the $H \to ZZ \to \ell\ell\nu\nu$ search for low mass ($m_H < 280$ GeV) and high mass ($m_H \geq 280$ GeV) selections. Electron and muon channels are combined. The expected signal events include minor additional contributions from $H \to ZZ \to \ell\ell qq$, $H \to ZZ^{(*)} \to \ell\ell\ell\ell$ and one which can be large from $H \to WW^{(*)} \to \ell\nu\ell\nu$. The uncertainties shown are the statistical and systematic uncertainties, respectively

Source	Low mass selection	High mass selection
Z + jets	$1.09 \pm 0.29 \pm 0.59$	$1.01 \pm 0.29 \pm 0.58$
W + jets	$1.07 \pm 0.31 \pm 0.64$	$0.41 \pm 0.19 \pm 0.22$
$t\bar{t}$	$1.90 \pm 0.10 \pm 0.63$	$0.91 \pm 0.07 \pm 0.31$
Multi-jet	$0.11 \pm 0.11 \pm 0.06$	–
ZZ	$0.58 \pm 0.01 \pm 0.11$	$0.51 \pm 0.01 \pm 0.10$
WZ	$0.57 \pm 0.01 \pm 0.10$	$0.45 \pm 0.01 \pm 0.09$
WW	$0.43 \pm 0.02 \pm 0.09$	$0.16 \pm 0.01 \pm 0.04$
Total background	$5.8 \pm 0.5 \pm 1.3$	$3.5 \pm 0.4 \pm 0.8$
$H \to ZZ \to \ell\ell\nu\nu$	$0.19 \pm (< 0.001) \pm 0.04$ ($m_H = 200$ GeV)	$0.30 \pm (< 0.001) \pm 0.06$ ($m_H = 400$ GeV)
Observed	5	5

the total expected signal yield. In particular, $H \to WW^{(*)} \to \ell\nu\ell\nu$ decays can lead to final states that are very similar to $H \to ZZ \to \ell\ell\nu\nu$ decays. They are found to contribute significantly to the signal yield at low m_H values. The expected number of events from $H \to WW^{(*)} \to \ell\nu\ell\nu$ decays relative to that from $H \to ZZ \to \ell\ell\nu\nu$ decays is 76% for $m_H = 200$ GeV and 9% for $m_H = 300$ GeV. The kinematic selections prevent individual candidates from being accepted by both searches. The E_T^{miss} distribution before vetoing events with low E_T^{miss} is shown in Fig. 7.
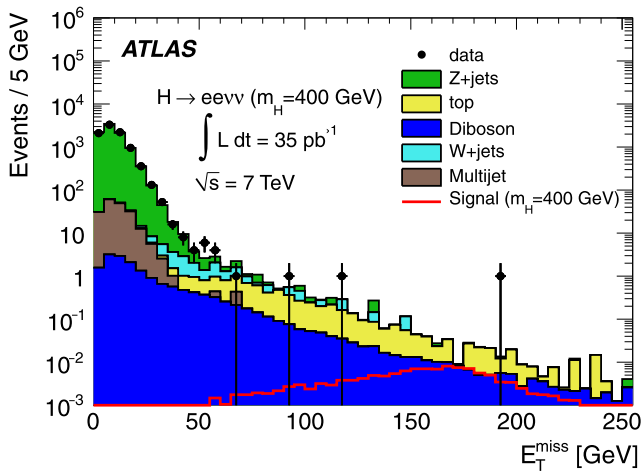

Fig. 7 Distribution of missing transverse energy in the $H \to ZZ \to \ell\ell\nu\nu$ search in the electron channel before vetoing events with low E_T^{miss}. The expected yield for a Higgs boson with $m_H = 400$ GeV is also shown. The distribution in the muon channel is similar with four events seen which have E_T^{miss} above 80 GeV

7 Combination method

The limit-setting procedure uses the power-constrained profile likelihood method known as the Power Constrained Limit, PCL [13, 14, 68]. This method is preferred to the more familiar CL_s [15] technique because the constraint is more transparently defined and it has reduced overcoverage resulting in a more precise meaning of the quoted confidence level. The resulting PCL median limits have been found to be around 20% tighter than those obtained with the CL_s method in several Higgs searches. The application of the PCL method to each of the individual Higgs boson search channels is described in Refs. [7–11]. A similar procedure is used here. The individual analyses are combined by maximising the product of the likelihood functions for each channel and computing a likelihood ratio. A single signal normalisation parameter μ is used for all analyses, where μ is the ratio of the hypothesised cross section to the expected Standard Model cross section.

Each channel has sources of systematic uncertainty, some of which are common with other channels. Table 7 lists the common sources of systematic uncertainties, which are taken to be 100% correlated with other channels. Let the search channels be labelled by l ($l = H \to \gamma\gamma$, $H \to WW$, ...), the background contribution, j, to channel l by j_l and the systematic uncertainties by i (i = luminosity, jet energy scale, ...). The relative magnitude of the effect on the Higgs boson signal yield in channel l due to systematic uncertainty i is then denoted by ϵ_{li}^s, and on background contribution j_l, ϵ_{jli}^b. The ϵ_{li}'s are constants; an individual ϵ_{li}^s can be zero

Table 7 Summary of systematic uncertainties (in percent) of the signal yield. The correlated systematic uncertainties are given in detail, the uncorrelated ones are lumped together. The uncertainties are evaluated for a Higgs boson mass of 115 GeV for the $H \to \gamma\gamma$ channel, 160 GeV for $H \to WW^{(*)} \to \ell\nu\ell\nu$, 200 GeV for the $H \to ZZ^{(*)} \to \ell\ell\ell\ell$ and 400 GeV for the remaining channels. Systematic errors

marked with a dash are neglected. In the three channels, the impact of the lepton energy scale and resolution uncertainties on the efficiency was found to be negligible, but they can still influence the fit via the signal distributions. In the $H \to WW \to \ell\nu qq$ channel a jet energy scale uncertainty can only decrease the efficiency; the resolution uncertainty is negligible in comparison

| | $\gamma\gamma$ | $H \to WW$ | | $H \to ZZ$ | | |
		$\ell\nu\ell\nu$	$\ell\nu qq$	$\ell\ell\ell\ell$	$\ell\ell\nu\nu$	$\ell\ell qq$
Luminosity	±3.4	±3.4	±3.4	±3.4	±3.4	±3.4
e/γ efficiency	± 11	±8.2	±2.6	±2.1	±4.6	±0.0
e/γ energy scale	–	±1.6	–	–	±0.5	±0.2
e/γ resolution	–	±1.6	–	–	±0.1	±0.1
μ efficiency	–	±0.5	±1.0	±0.8	±0.0	±2.0
μ energy scale	–	±4.8	–	–	±1.2	$+0.2 \atop -2.2$
μ resolution	–	±1.2	–	–	±0.1	±0.1
Jet energy scale	–	±3.7	−26	–	±0.4	$+2.9 \atop -7.0$
Jet energy resolution	–	–	–	–	±0.2	$+0.0 \atop -1.3$
b-tag efficiency	–	–	–	–	±0.4	–
Uncorrelated	±10	±5.0	–	–	–	–

if the channel in question is not affected by this source of systematic uncertainty. A common systematic uncertainty, i, which is shared between channels l and l' implies that ϵ_{li}^s and $\epsilon_{l'i}^s$ are both different from zero. If a systematic source i is shared between the signal in channel l and background contribution j_l then both ϵ_{li}^s and ϵ_{jli}^b are non-zero. For each source of systematic uncertainty i there is a corresponding nuisance parameter δ_i and an associated auxiliary measurement m_i on a control sample (e.g. sidebands in a mass spectrum) that is used to constrain the parameter. The δ_i and m_i are scaled so that $\delta_i = 0$ corresponds to the nominal expectation and $\delta_i = \pm 1$ corresponds to the $\pm 1\sigma$ variations of the source. When constructing ensembles for statistical evaluation, each m_i is sampled according to $G(m_i|\delta_i, 1)$, the standard normal distribution. Using this notation, the total number of expected events in the signal region for channel l is given by:

$$
\begin{aligned}
N_l^{\exp} = &\mu L \sigma_l \prod_i \left(1 + \epsilon_{li}^s \delta_i\right) \\
&+ \sum_j b_{jl} \prod_i \left(1 + \epsilon_{jli}^b \delta_i\right)
\end{aligned}
\tag{2}
$$

for luminosity L, Standard Model cross sections σ_l (including efficiencies and acceptances), and expected backgrounds b_{jl}. Background estimates b_{jl} may come either from Monte Carlo simulations or from control regions in which the expected number of events, $\bar{n}_{jl}$, is proportional to the expected background, via $b_{jl} = \alpha_{jl} \bar{n}_{jl}$. Given the number of observed events in the signal region N_l^{obs}, the likelihood function can be written as:

$$
\mathcal{L}_l = \mathrm{Pois}\left(N_l^{\mathrm{obs}}|N_l^{\exp}\right) \prod_{j_l} \mathrm{Pois}(n_{jl}|\bar{n}_{jl}) \prod_i G(m_i|\delta_i, 1),
$$

where n_{jl} are the observed numbers of background events in the control regions and $\mathrm{Pois}(x|y)$ is the Poisson probability of observing x events given an expectation y.

The combined likelihood is given by the product of the individual likelihoods for each channel:

$$
\mathcal{L} = \prod_l \mathcal{L}_l,
$$

where l is implicitly an index over the individual histogram bins within the channels that used a binned distribution of a discriminating variable.

The profile likelihood ratio

$$
\tilde{\lambda}(\mu) =
\begin{cases}
\dfrac{\mathcal{L}(\mu, \hat{\hat{\theta}}(\mu))}{\mathcal{L}(\hat{\mu}, \hat{\theta})}, & \hat{\mu} \geq 0, \\[2ex]
\dfrac{\mathcal{L}(\mu, \hat{\hat{\theta}}(\mu))}{\mathcal{L}(0, \hat{\hat{\theta}}(0))}, & \hat{\mu} < 0,
\end{cases}
\tag{3}
$$

is computed by maximising the likelihood function twice: in the numerator μ, the ratio of the hypothesised cross section to the expected Standard Model cross section, is restricted to a particular value and in the denominator μ is allowed to float. The set of all nuisance parameters δ_i and $\bar{n}_{jl}$ is denoted θ. The maximum likelihood estimates of μ and θ are denoted $\hat{\mu}$ and $\hat{\theta}$, while $\hat{\hat{\theta}}(\mu)$ denotes the conditional maximum likelihood estimate of all nuisance parameters with μ fixed. In this analysis the range of μ is restricted to the physically meaningful regime, i.e. it is not allowed to be negative. The test statistic $\tilde{q}_\mu$ is defined to be

$$
\begin{aligned}
\tilde{q}_\mu &=
\begin{cases}
-2\ln \tilde{\lambda}(\mu), & \hat{\mu} \leq \mu, \\
0, & \hat{\mu} > \mu,
\end{cases} \\[2ex]
&=
\begin{cases}
-2\ln \dfrac{\mathcal{L}(\mu, \hat{\hat{\theta}}(\mu))}{\mathcal{L}(0, \hat{\hat{\theta}}(0))}, & \hat{\mu} < 0, \\[2ex]
-2\ln \dfrac{\mathcal{L}(\mu, \hat{\hat{\theta}}(\mu))}{\mathcal{L}(\hat{\mu}, \hat{\theta})}, & 0 \leq \hat{\mu} \leq \mu, \\[2ex]
0, & \hat{\mu} > \mu.
\end{cases}
\end{aligned}
\tag{4}
$$

Monte Carlo pseudo-experiments are generated to construct the probability density function $f(\tilde{q}_\mu|\mu, \hat{\hat{\theta}}(\mu))$ under an assumed signal strength μ, giving a p-value

$$
p_\mu = \int_{\tilde{q}_{\mu,\mathrm{obs}}}^{\infty} f(\tilde{q}_\mu|\mu, \hat{\hat{\theta}}(\mu)) \, \mathrm{d}\tilde{q}_\mu.
\tag{5}
$$

To find the upper limit on μ at 95% confidence level, μ_{up}, μ is varied to find $p_{\mu_{\mathrm{up}}} = 5\%$. Similarly, background-only Monte Carlo pseudo-experiments are used to find the median μ_{med} along with the $\pm 1\sigma$ and $+2\sigma$ bands expected in the absence of a signal. The procedure so far can be referred to as a CL_{sb} limit. To protect against excluding the (signal) null hypothesis in cases of downward fluctuations of the background, the observed limit is not allowed to fluctuate below the -1σ expected limit. This is equivalent to restricting the interval to cases in which the statistical power of the test of μ against the alternative $\mu = 0$ is at least 16%. This is referred to as a Power Constrained Limit. If the observed limit fluctuates below the 16% power, the quoted limit is $\mu_{\mathrm{med}} - 1\sigma$.

8 Systematic uncertainties in the combination

The systematic uncertainty related to the luminosity is $\pm 3.4\%$ and is fully correlated among all channels. It affects background estimates that are normalised to their theoretical cross sections; for most channels this is only true for backgrounds that are known to be small. In the $H \to ZZ \to \ell\ell\nu\nu$ and $H \to ZZ \to \ell\ell qq$ channels major backgrounds are normalised to their theoretical cross sections, but in the latter case this is only done after comparing with control regions.

Sources of systematic uncertainty related to the event reconstruction are correlated between all the Higgs boson search channels. The uncertainty on the efficiency to reconstruct electrons varies between 2.5% (central high-p_T elec-

trons) and 16% (p_T near 15 GeV, the lowest value used here) but it is assumed to be completely correlated. For muons the efficiency uncertainty ranges between 0.4% and 2%. The jet systematic errors are typically larger for the channels where jets are explicitly required. They are dominated by the jet energy scale as the resolution effects tend to partially cancel and the E_T^{miss} uncertainties are largely by-products of the uncertainties already discussed.

The effect on the signal yield in each channel of the major sources of systematic uncertainty is summarised in Table 7. Uncertainties are treated as either uncorrelated or 100% correlated among channels. The largest uncorrelated errors are photon isolation in $H \to \gamma\gamma$ and jet rates in $H \to WW^{(*)} \to \ell\nu\ell\nu$; the latter is in principle correlated with the $H \to WW \to \ell\nu qq$ channel but these channels are never used in the same mass region. Most backgrounds have been estimated by means of independent control samples; these estimates are assumed to be uncorrelated between the channels.

Systematic uncertainties on the signal shape are accounted for in the $H \to \gamma\gamma$, $H \to ZZ \to \ell\ell qq$ and $H \to ZZ \to \ell\ell\nu\nu$ channels by considering three possible distributions and interpolating between them. Small signal shape systematic uncertainties in the $H \to ZZ^{(*)} \to \ell\ell\ell\ell$ and $H \to WW \to \ell\nu qq$ channels are neglected. For $m_H \geq 200$ GeV the correlations in the shape systematics are taken into account and are treated as correlated with the signal normalisation uncertainties.

The width of the Higgs boson signal at high mass is taken from the PYTHIA Monte Carlo [53]. This underestimates the width and the accepted cross section is conservatively scaled down by the ratio of the widths given in Ref. [69], which reached a maximum of 8% at 600 GeV, in all plots showing a ratio to the Standard Model.

The systematic uncertainty coming from the total theoretical Higgs boson cross section is not included in the combination and is shown separately in the figures as an uncertainty on the predicted cross section.

9 Combination

Each Higgs boson search channel is only sensitive for a range of Higgs boson masses. The ranges in which the various channels have been analysed are detailed in Table 8.

Table 8 The Higgs boson mass regions in which individual search channels have been analysed

Mode	Mass range, GeV
$H \to \gamma\gamma$	110–140
$H \to WW^{(*)} \to \ell\nu\ell\nu$	120–200
$H \to WW \to \ell\nu qq$	220–600
$H \to ZZ^{(*)} \to \ell\ell\ell\ell$	120–600
$H \to ZZ \to \ell\ell\nu\nu$	200–600
$H \to ZZ \to \ell\ell qq$	200–600
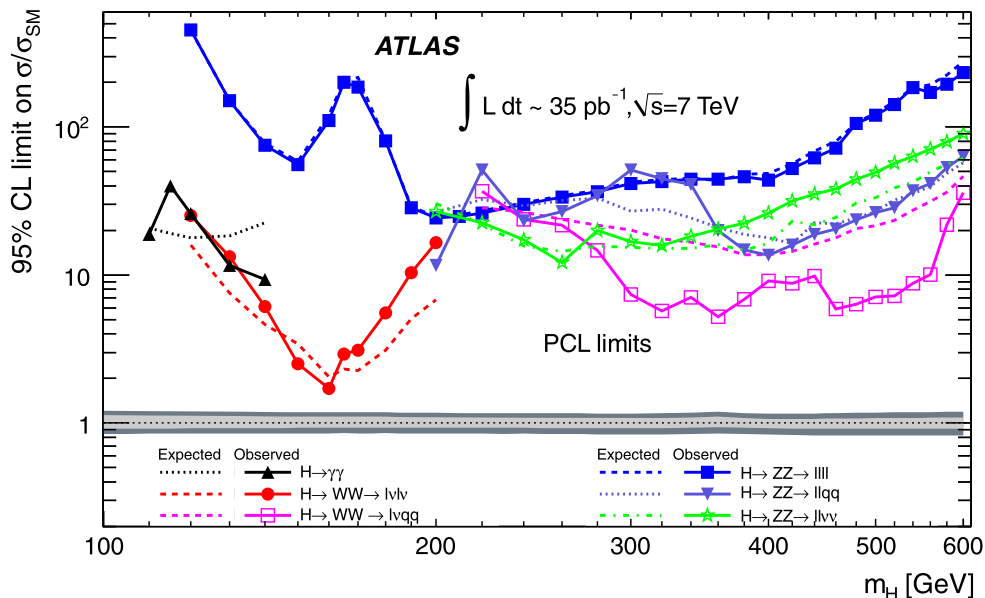
Fig. 8 The expected and observed cross section limits, normalized to the Standard Model cross section, as a function of the Higgs boson mass for the individual search channels. The visually most apparent difference between expected and observed is in the $H \to WW \to \ell\nu qq$ channel, which has a deficit approaching one sigma both at 320 GeV and 480 GeV. These results use the profile likelihood method with a power constraint (PCL). The limits are calculated at the masses marked with symbols. The lines between the points are to guide the eye. The *grey horizontal bands* show the uncertainty on the Standard Model cross section prediction, with the inner region highlighting the contribution of QCD scale uncertainties

In the $H \to \gamma\gamma$, $H \to ZZ \to \ell\ell\nu\nu$ and $H \to ZZ \to \ell\ell qq$ channels, the final result is extracted from a fit of signal plus background contributions to the observed Higgs boson candidate mass distributions. In all other channels, limits are extracted from a comparison of the numbers of observed events in one or more signal regions to the numbers of estimated background events.

The individual channels are shown in Fig. 8 in terms of the observed and the expected upper limits on σ/σ_{SM} at the 95% confidence level. The step with which the limit is extracted, 5–10 GeV, does not match the $H \to \gamma\gamma$ resolution which has a full-width at half maximum of 4.4 GeV. However, it was established in Ref. [7] that no important fluctuations are missed.

The search channels are grouped by the primary Higgs boson decay mode searched for, $\gamma\gamma$, WW or ZZ, and the limit on each mode is extracted in terms of the cross section for the process intended. Some channels have a contribution from signal modes other then the intended one. This is only significant for the $H \to ZZ \to \ell\ell\nu\nu$ search, as discussed in Sect. 6.3, and implies that the ZZ limit assumes the Standard Model ratio between H to ZZ and H to WW decays. In addition, the WW search requires zero or one jet and is essentially designed for a spin-zero object produced largely via gluon fusion. The upper limits at 95% confidence level observed and expected in the absence of a signal are compared with the cross section expected for a Standard Model Higgs boson in Fig. 9.

Fig. 9 The expected and observed 95% PCL limits on the total cross section of a particle produced like the Standard Model Higgs boson and decaying with the width predicted by PYTHIA[53] to pairs of bosons: $\gamma\gamma$, WW or ZZ. The limits are calculated at the masses marked with symbols. The lines between the points are to guide the eye. The *coloured bands* show the cross section predictions and their uncertainties, with the inner region highlighting the contribution of QCD scale uncertainties
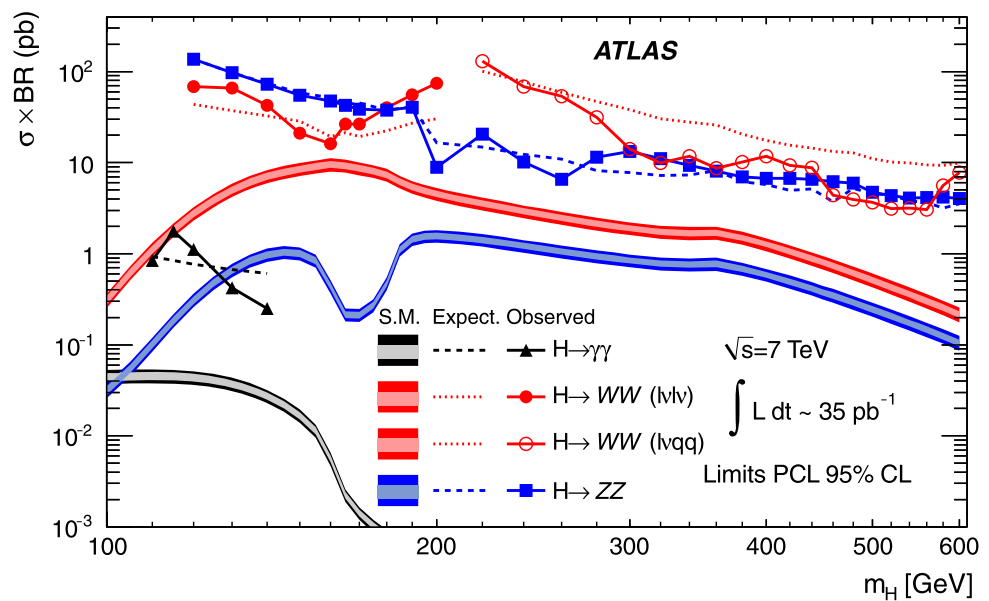
Fig. 10 The expected and observed upper limits on the total cross section divided by the expected Standard Model Higgs boson cross section. This is a 95% PCL limit. The *green* and *yellow bands* indicate the range in which the limit is expected to lie in the absence of a signal. The *fine dotted line* marks the results obtained using CL_{sb}, and the application of the power constraint gives the *solid line*. The limits are calculated at the masses marked with symbols and the lines between the points are to guide the eye
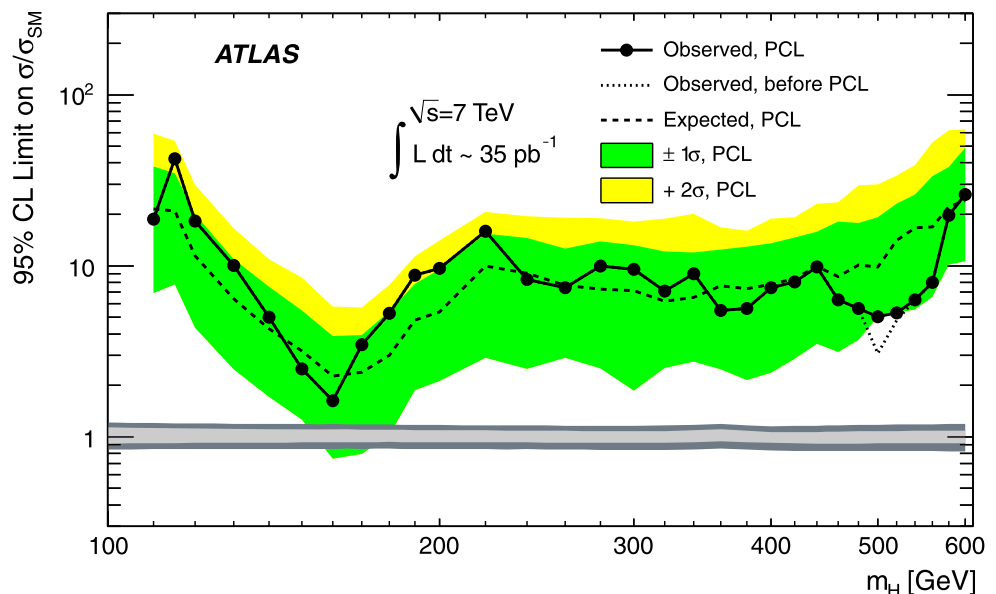
Table 9 The signal cross sections, in multiples of the Standard Model cross section, that are excluded, and expected to be excluded, at 95% CL. The expected variation at $\pm 1\sigma$ is also given for the PCL limits. The bold numbers show the limit which should be used; for mass of 500 and 520 GeV the power constraint is applied. The likelihood ratio of signal plus background to background is also shown, as is the p-value (modified to go between 0 and 1) for $\mu = 0$, which can be used to estimate the discovery significance

| m_H (GeV) | PCL limits | | | | CL_s limits | | $-2\ln\frac{\mathcal{L}(1,\hat{\hat{\theta}})}{\mathcal{L}(0,\hat{\theta})}$ | p-values |
	Obs.	-1σ	Median	$+1\sigma$	Obs.	Median		$p_{\mu=0}$
110	**18.7**	6.9	21.5	38.2	28.1	29.6	0.1	0.58
115	**42.4**	7.8	20.9	34.7	43.5	25.3	−0.3	0.07
120	**18.2**	4.3	11.4	19.9	19.7	15.4	−0.3	0.22
130	**10.0**	2.5	6.4	10.9	11.0	8.5	−0.6	0.23
140	**5.0**	1.7	4.3	7.6	6.1	5.9	0.0	0.41
150	**2.5**	1.3	3.2	5.5	4.0	4.4	1.0	0.65
160	**1.6**	0.7	2.3	3.9	2.8	3.1	1.6	0.68
170	**3.4**	0.8	2.4	3.9	3.8	3.1	−0.4	0.27
180	**5.3**	1.0	3.0	5.4	5.6	4.2	−0.9	0.18
190	**8.8**	1.9	4.8	7.8	9.2	6.3	−1.1	0.11
200	**9.7**	2.1	5.4	9.5	9.9	7.5	−1.1	0.15
220	**15.9**	2.9	10.0	15.4	17.1	12.9	0.0	0.13
240	**8.3**	2.5	9.1	14.5	11.2	11.9	0.3	0.57
260	**7.4**	2.9	7.7	12.6	10.8	10.9	0.4	0.56
280	**10.0**	2.5	7.3	13.9	11.5	10.2	0.2	0.31
300	**9.5**	1.9	7.2	13.2	11.4	10.1	0.2	0.32
320	**7.1**	2.5	6.2	12.1	9.8	9.5	0.4	0.40
340	**9.0**	2.8	6.5	11.9	9.9	9.6	0.4	0.28
360	**5.5**	2.5	7.7	12.5	8.5	9.5	0.4	0.63
380	**5.6**	2.2	7.3	12.9	8.6	9.5	0.4	0.53
400	**7.5**	2.4	7.8	13.6	9.4	9.6	0.1	0.49
420	**8.0**	2.9	8.4	14.7	10.4	10.4	0.2	0.46
440	**9.8**	3.5	9.9	15.8	11.7	11.8	0.1	0.46
460	**6.3**	3.1	8.7	18.1	10.1	12.3	0.4	0.64
480	**5.6**	3.7	10.1	17.7	10.4	13.4	0.4	0.80
500	3.1	**5.0**	9.9	19.3	11.8	15.9	0.5	0.89
520	4.8	**5.3**	14.1	23.1	13.9	18.5	0.4	0.86
540	**6.3**	5.6	16.7	26.0	16.8	21.3	0.4	0.82
560	**8.0**	6.6	16.9	33.5	19.3	23.7	0.3	0.80
580	**19.7**	10.2	22.2	37.9	27.5	28.8	0.1	0.56
600	**26.1**	10.6	24.0	49.2	34.4	33.9	0.1	0.45

Fig. 11 Same as Fig. 10, except that limits calculated using the CL_s procedure are added. As expected, when the observed limits fluctuate up, both methods converge, but downward fluctuations are less pronounced with CL_s due to its larger over-coverage. The fine dotted line marks the results obtained using CL_{sb}, and the application of the power constraint gives the solid line. The limits are calculated at the masses marked with symbols. The lines between the points are to guide the eye. The regions excluded by the combined LEP experiments [4] and the Tevatron experiments [6] are indicated
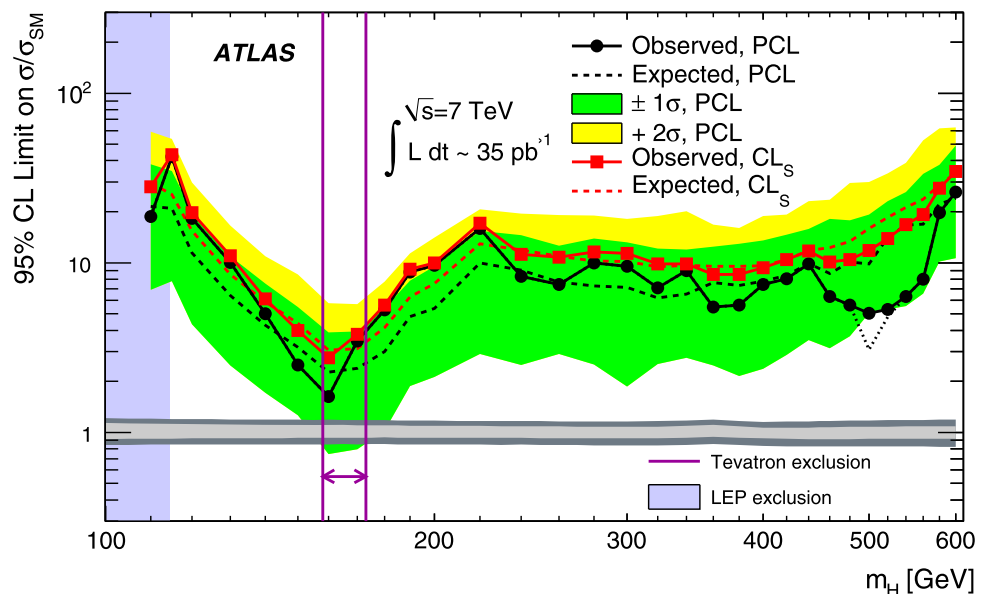
Fig. 12 Same as Fig. 10, but comparing the excluded cross section to the expected one when a fourth generation of high mass quarks and leptons with Standard Model-like couplings to the Higgs boson are included in the cross section calculations. The arrows indicate the regions excluded by the CMS experiment [12] and the Tevatron experiments [70]. The point set at 500 GeV is at the limit allowed by the power constraint. The limits are calculated at the masses marked with symbols. The lines between the points are to guide the eye
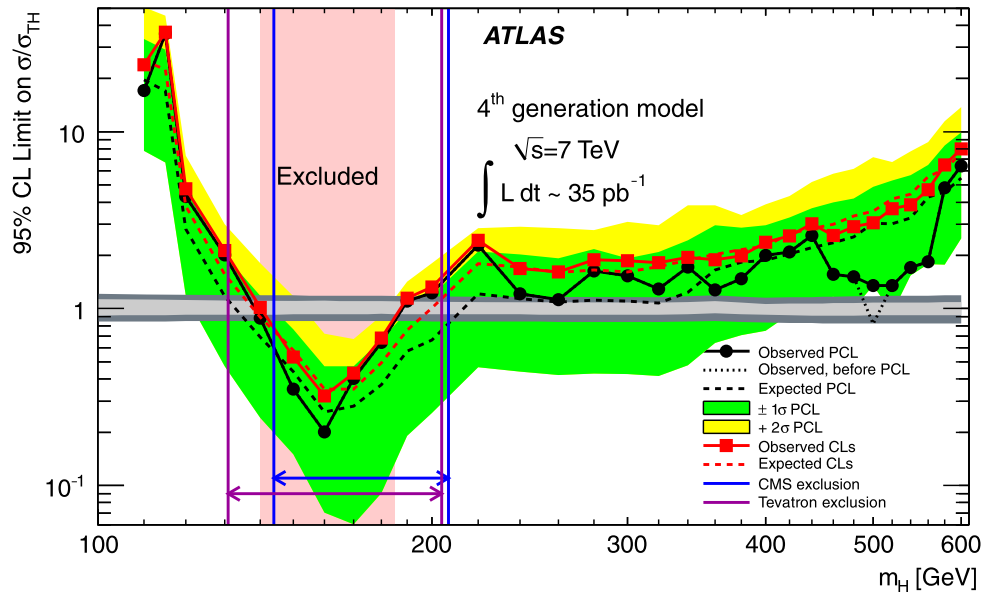

Table 10 The signal cross sections, in multiples of the high mass fourth generation model [50] cross section, that are excluded, and expected to be excluded, in the absence of signal, at 95% CL

m_H (GeV)	PCL limits			CL_s limits		m_H (GeV)	PCL limits			CL_s limits	
	Obs.	-1σ	Median	Median	Obs.		Obs.	-1σ	Median	Median	Obs.
110	**17.1**	7.8	19.6	25.2	23.9	320	**1.3**	0.4	1.1	1.7	1.8
115	**35.8**	6.7	17.0	22.4	36.6	340	**1.7**	0.5	1.2	1.9	1.9
120	**4.3**	1.2	2.8	3.8	4.8	360	**1.3**	0.6	1.7	2.0	1.9
130	**2.0**	0.5	1.2	1.6	2.1	380	**1.5**	0.7	1.8	2.1	2.0
140	**0.9**	0.2	0.7	0.9	1.0	400	**2.0**	0.8	1.9	2.2	2.3
150	**0.4**	0.2	0.4	0.6	0.5	420	**2.1**	0.9	2.0	2.6	2.5
160	**0.2**	0.1	0.3	0.4	0.3	440	**2.6**	1.1	2.2	2.8	3.0
170	**0.4**	0.1	0.3	0.4	0.4	460	**1.6**	1.2	2.4	3.0	2.6
180	**0.6**	0.1	0.4	0.5	0.7	480	**1.5**	1.0	2.5	3.3	2.9
190	**1.1**	0.2	0.6	0.8	1.1	500	0.8	**1.4**	3.0	3.5	3.0
200	**1.2**	0.3	0.7	1.0	1.3	520	**1.3**	0.9	3.0	4.1	3.6
220	**2.3**	0.5	1.2	1.8	2.4	540	**1.7**	1.5	3.3	4.3	3.8
240	**1.2**	0.4	1.1	1.7	1.7	560	**1.8**	1.8	4.3	5.4	4.6
260	**1.1**	0.4	1.1	1.6	1.6	580	**4.8**	1.8	4.6	6.0	6.3
280	**1.6**	0.4	1.1	1.6	1.9	600	**6.4**	2.5	5.5	7.4	7.8
300	**1.5**	0.4	1.1	1.6	1.9						

The combination of all channels is tested and the $p_{\mu=0}$ in these fits varies between 7% and 89%, which does not suggest the presence of a signal. The combination of all channels is shown in Fig. 10 in terms of the observed and the expected upper limit at the 95% confidence level. The statistical accuracy of the toy Monte Carlo used to extract the limits is about 5% on the observed limits and 7% on the expected ones, with somewhat larger variation on the edges of the one and two σ bands.

The excluded signal strength as a function of m_H is summarised in Table 9, using the PCL method. The results are also calculated using the CL_s method for comparison pur-

poses: the extracted limits from both procedures are shown in Fig. 11. Also given is the profile likelihood ratio of a Standard Model Higgs boson to background only and the consistency of the data with the background-only hypothesis, $p_{\mu=0}$.

The results have been interpreted in terms of the heavy mass fourth generation model introduced in Sect. 3. This involves rescaling the gluon fusion component of the production cross section and the Higgs boson decay branching ratios. The limits are shown in Fig. 12. This model is excluded for Higgs boson masses between 140 GeV and 185 GeV,

while the region in which exclusion might be expected is between 136 GeV and 208 GeV.

The excluded cross section ratios are summarised in Table 10.

10 Conclusions

The ATLAS search for the Standard Model Higgs boson in the mass range from 110 GeV to 600 GeV in 35 to 40 pb^{-1} of data recorded in 2010 has been presented. With this luminosity there is not sufficient sensitivity to exclude the Standard Model Higgs boson, nor is there any evidence of an excess of events over the predicted background rates. However, these results give the most stringent constraints to date for Higgs boson masses above 250 GeV and are close to the Tevatron limits [6] at intermediate masses.

An extension of the Standard Model, assuming the Higgs mechanism and adding a fourth generation of heavy quarks and leptons, is excluded for Higgs boson masses between 140 and 185 GeV.

References

1. F. Englert, R. Brout, Broken symmetry and the mass of gauge vector mesons. Phys. Rev. Lett. **13**, 321–323 (1964)

2. P.W. Higgs, Broken symmetries, massless particles and gauge fields. Phys. Lett. **12**, 132–133 (1964)

3. G. Guralnik, C. Hagen, T. Kibble, Global conservation laws and massless particles. Phys. Rev. Lett. **13**, 585–587 (1964)

4. R. Barate, et al. (LEP Working Group for Higgs boson searches), Search for the standard model Higgs boson at LEP. Phys. Lett. B **565**, 61–75 (2003)

5. The TEVNPH Working Group of the CDF and D0 Collaboration, Combined CDF and D0 upper limits on standard model Higgs-boson production with up to 6.7 fb^{-1} of data. arXiv:1007.4587 [hep-ex]

6. The TEVNPH Working Group of the CDF and D0 Collaboration, Combined CDF and D0 upper limits on standard model Higgs-boson production with up to 8.2 fb^{-1} of data. arXiv:1103.3233 [hep-ex]

7. ATLAS Collaboration, Search for the Higgs boson in the diphoton final state with 38 pb^{-1} of data recorded by the ATLAS detector in proton-proton collisions at $\sqrt{s} = 7$ TeV. ATLAS-CONF-2011-025

8. ATLAS Collaboration, Higgs boson searches using the $H \to WW^{(*)} \to \ell\nu\ell\nu$ decay mode with the ATLAS detector at 7 TeV. ATLAS-CONF-2011-005

9. ATLAS Collaboration, Search for Higgs boson production in pp collisions at $\sqrt{s} = 7$ TeV using the $H \to WW \to l\nu qq$ decay channel and the ATLAS detector. ATLAS-CONF-2011-052

10. ATLAS Collaboration, Search for the standard model Higgs boson in the decay channel $H \to ZZ^{(*)} \to 4\ell$ with 40 pb^{-1} of pp collisions at $\sqrt{s} = 7$ TeV. ATLAS-CONF-2011-048

11. ATLAS Collaboration, Search for a standard model Higgs boson in the mass range 200–600 GeV in the channels $H \to ZZ \to \ell^+\ell^-\nu\bar{\nu}$ and $H \to ZZ \to \ell^+\ell^-q\bar{q}$ with the ATLAS detector. ATLAS-CONF-2011-026

12. CMS Collaboration, Measurement of WW production and search for the Higgs boson in pp collisions at $\sqrt{s} = 7$ TeV. Phys. Lett. B **699**, 25–47 (2011)

13. ATLAS Collaboration, Expected performance of the ATLAS experiment—detector, trigger and physics. arXiv:0901.0512 [hep-ex] (p. 1480)

14. G. Cowan, K. Cranmer, E. Gross, O. Vitels, Power-constrained limits. arXiv:1105.3166 [hep-ph]

15. A.L. Read, Presentation of search results: The CL(s) technique. J. Phys. G **28**, 2693–2704 (2002)

16. ATLAS Collaboration, The ATLAS experiment at the CERN large hadron collider. J. Instrum. **3**, S08003 (2008)

17. ATLAS Collaboration, Updated luminosity determination in pp collisions at $\sqrt{s} = 7$ TeV using the ATLAS detector. ATLAS-CONF-2011-011

18. ATLAS Collaboration, Measurement of inclusive jet and dijet cross sections in proton-proton collisions at 7 TeV centre-of-mass energy with the ATLAS detector. Eur. Phys. J. C **71**, 1512 (2011)

19. M. Cacciari, G.P. Salam, G. Soyez, The anti-k_T jet clustering algorithm. J. High Energy Phys. **04**, 063 (2008). arXiv:0802.1189 [hep-ph]

20. ATLAS Collaboration, Jet energy scale and its systematic uncertainty in proton-proton collisions at $\sqrt{s} = 7$ TeV in ATLAS 2010 data. ATLAS-CONF-2011-032

21. S. Dittmaier, C. Mariotti, G. Passarino, R. Tanaka (LHC Higgs Cross Section Working Group) (eds.), *Handbook of LHC Higgs Cross Sections: 1. Inclusive Observables* (CERN, Geneva, 2011). CERN-2011-002. arXiv:1101.0593 [hep-ph]

22. R.V. Harlander, W.B. Kilgore, Next-to-next-to-leading order Higgs production at hadron colliders. Phys. Rev. Lett. **88**, 201801 (2002)

23. C. Anastasiou, K. Melnikov, Higgs boson production at hadron colliders in NNLO QCD. Nucl. Phys. B **646**, 220–256 (2002)

24. V. Ravindran, J. Smith, W.L. van Neerven, NNLO corrections to the total cross section for Higgs boson production in hadron hadron collisions. Nucl. Phys. B **665**, 325–366 (2003)

25. C. Anastasiou, R. Boughezal, F. Petriello, Mixed QCD-electroweak corrections to Higgs boson production in gluon fusion. J. High Energy Phys. **04**, 003 (2009)

26. D. de Florian, M. Grazzini, Higgs production through gluon fusion: Updated cross sections at the Tevatron and the LHC. Phys. Lett. B **674**, 291–294 (2009)

27. J. Baglio, A. Djouadi, Higgs production at the lHC. J. High Energy Phys. **1103**, 055 (2011)

28. P. Bolzoni, F. Maltoni, S.-O. Moch, M. Zaro, Higgs production via vector-boson fusion at NNLO in QCD. Phys. Rev. Lett. **105**, 011801 (2010)

29. O. Brein, A. Djouadi, R. Harlander, NNLO QCD corrections to the Higgs-Strahlung processes at hadron colliders. Phys. Lett. B **579**, 149–156 (2004)

30. W. Beenakker et al., Higgs radiation off top quarks at the Tevatron and the LHC. Phys. Rev. Lett. **87**, 201805 (2001)

31. S. Dawson, L.H. Orr, L. Reina, D. Wackeroth, Associated top quark Higgs boson production at the LHC. Phys. Rev. D **67**, 071503 (2003)

32. S. Catani, D. de Florian, M. Grazzini, P. Nason, Soft-gluon resummation for Higgs boson production at hadron colliders. J. High Energy Phys. **07**, 028 (2003)

33. U. Aglietti, R. Bonciani, G. Degrassi, A. Vicini, Two-loop light fermion contribution to Higgs production and decays. Phys. Lett. B **595**, 432–441 (2004)

34. S. Actis, G. Passarino, C. Sturm, S. Uccirati, NLO electroweak corrections to Higgs boson production at hadron colliders. Phys. Lett. B **670**, 12–17 (2008)

35. M. Ciccolini, A. Denner, S. Dittmaier, Strong and electroweak corrections to the production of Higgs +2 jets via weak interactions at the LHC. Phys. Rev. Lett. **99**, 161803 (2007)

36. M. Ciccolini, A. Denner, S. Dittmaier, Electroweak and QCD corrections to Higgs production via vector-boson fusion at the LHC. Phys. Rev. D **77**, 013002 (2008)

37. M.L. Ciccolini, S. Dittmaier, M. Krämer, Electroweak radiative corrections to associated WH and ZH production at hadron colliders. Phys. Rev. D **68**, 073003 (2003)

38. A. Djouadi, J. Kalinowski, M. Spira, HDECAY: A program for Higgs boson decays in the standard model and its supersymmetric extension. Comput. Phys. Commun. **108**, 56–74 (1998)

39. A. Bredenstein, A. Denner, S. Dittmaier, M.M. Weber, Precise predictions for the Higgs-boson decay $H \rightarrow WW/ZZ \rightarrow 4$ leptons. Phys. Rev. D **74**, 013004 (2006)

40. A. Bredenstein, A. Denner, S. Dittmaier, M. Weber, Radiative corrections to the semileptonic and hadronic Higgs-boson decays $H \rightarrow WW/ZZ \rightarrow 4$ fermions. J. High Energy Phys. **0702**, 080 (2007)

41. K. Nakamura et al. (Particle Data Group), Review of particle physics. J. Phys. G **37**, 075021 (2010)

42. M. Botje, J. Butterworth, A. Cooper-Sarkar, A. de Roeck, J. Feltesse et al., The PDF4LHC working group interim recommendations. arXiv:1101.0538 [hep-ph]

43. R.D. Ball, V. Bertone, F. Cerutti, L. Del Debbio, S. Forte et al., Impact of heavy quark masses on parton distributions and LHC phenomenology. Nucl. Phys. B **849**, 296–363 (2011)

44. H.-L. Lai, M. Guzzi, J. Huston, Z. Li, P.M. Nadolsky et al., New parton distributions for collider physics. Phys. Rev. D **82**, 074024 (2010). arXiv:1007.2241 [hep-ph]

45. A.D. Martin, W.J. Stirling, R.S. Thorne, G. Watt, Parton distributions for the LHC. Eur. Phys. J. C **63**, 189–285 (2009). arXiv:0901.0002 [hep-ph]

46. G.D. Kribs, T. Plehn, M. Spannowsky, T.M. Tait, Four generations and Higgs physics. Phys. Rev. D **76**, 075016 (2007). arXiv:0706.3718 [hep-ph]

47. N. Schmidt, S. Cetin, S. Istin, S. Sultansoy, The fourth standard model family and the competition in standard model Higgs boson search at Tevatron and LHC. Eur. Phys. J. C **66**, 119–126 (2010)

48. C. Anastasiou, R. Boughezal, E. Furlan, The NNLO gluon fusion Higgs production cross-section with many heavy quarks. J. High Energy Phys. **1006**, 101 (2010). arXiv:1003.4677 [hep-ph]

49. Q. Li, M. Spira, J. Gao, C.S. Li, Higgs boson production via gluon fusion in the standard model with four generations. Phys. Rev. D **83**, 094018 (2011). arXiv:1011.4484 [hep-ph]

50. X. Ruan, Z. Zhang, Impact on the Higgs production cross section and decay branching fractions of heavy quarks and leptons in a fourth generation model. arXiv:1105.1634 [hep-ph]

51. A. Rozanov, M. Vysotsky, Tevatron constraints on the Higgs boson mass in the fourth-generation fermion models revisited. Phys. Lett. B **700**, 313–315 (2011). arXiv:1012.1483 [hep-ph]

52. M. Spira, HIGLU: A program for the calculation of the total Higgs production cross section at hadron colliders via gluon fusion including QCD corrections. arXiv:hep-ph/9510347

53. T. Sjostrand, S. Mrenna, P.Z. Skands, PYTHIA 6.4 physics and manual. J. High Energy Phys. **0605**, 026 (2006)

54. P. Golonka, Z. Was, PHOTOS Monte Carlo: A precision tool for QED corrections in Z and W decays. Eur. Phys. J. C **45**, 97–107 (2006)

55. S. Frixione, B.R. Webber, Matching NLO QCD computations and parton shower simulations. J. High Energy Phys. **06**, 02 (2002)

56. S. Frixione, P. Nason, B.R. Webber, Matching NLO QCD and parton showers in heavy flavour production. J. High Energy Phys. **08**, 007 (2003)

57. T. Gleisberg et al., Event generation with SHERPA 1.1. J. High Energy Phys. **02**, 007 (2009). 0811.4622

58. G. Corcella et al., HERWIG 6.5 release note. arXiv:hep-ph/0210213

59. M.L. Mangano, M. Moretti, F. Piccinini, R. Pittau, A.D. Polosa, ALPGEN, a generator for hard multiparton processes in hadronic collisions. J. High Energy Phys. **07**, 001 (2003)

60. J. Alwall et al., MadGraph/MadEvent v4: The new web generation. J. High Energy Phys. **09**, 028 (2007)

61. ATLAS Collaboration, The ATLAS simulation infrastructure. Eur. Phys. J. C **70**, 823–874 (2010)

62. S. Agostinelli et al., (GEANT4 Collaboration), GEANT4: A simulation toolkit. Nucl. Instrum. Methods A **506**, 250–303 (2003)

63. ATLAS Collaboration, Measurement of the inclusive isolated prompt photon cross section in pp collisions at $\sqrt{s} = 7$ TeV with the ATLAS detector. Phys. Rev. D **83**, 052005 (2011)

64. B. Aubert et al. (BABAR Collaboration), Search for the rare Decay $B^0 \rightarrow \tau^+ \tau^-$ at BABAR. Phys. Rev. Lett. **96**(24), 241802 (2006)

65. M. Dittmar, H.K. Dreiner, How to find a Higgs boson with a mass between 155-GeV–180-GeV at the LHC. Phys. Rev. D **55**, 167–172 (1997)

66. A.J. Barr, B. Gripaios, C.G. Lester, Measuring the Higgs boson mass in dileptonic W-boson decays at hadron colliders. J. High Energy Phys. **07**, 072 (2009)

67. J.M. Campbell, E. Castaneda-Miranda, Y. Fang, N. Kauer, B. Mellado, S.L. Wu, Normalizing weak boson pair production at the large hadron collider. Phys. Rev. D **80**(5), 054023 (2009)

68. G. Cowan, K. Cranmer, E. Gross, O. Vitells, Asymptotic formulae for likelihood-based tests of new physics. Eur. Phys. J. C **71**, 1–19 (2011)

69. A. Djouadi, The anatomy of electro-weak symmetry breaking. I: The Higgs boson in the standard model. Phys. Rep. **457**, 1–216 (2008)

70. CDF and D0 Collaborations, Combined Tevatron upper limit on $gg \rightarrow H \rightarrow W^+ W^-$ and constraints on the Higgs boson mass in fourth-generation fermion models. Phys. Rev. D **82**, 011102 (2010)

The ATLAS Collaboration

G. Aad[48], B. Abbott[111], J. Abdallah[11], A.A. Abdelalim[49], A. Abdesselam[118], O. Abdinov[10], B. Abi[112], M. Abolins[88], H. Abramowicz[153], H. Abreu[115], E. Acerbi[89a,89b], B.S. Acharya[164a,164b], D.L. Adams[24], T.N. Addy[56], J. Adelman[175], M. Aderholz[99], S. Adomeit[98], P. Adragna[75], T. Adye[129], S. Aefsky[22], J.A. Aguilar-Saavedra[124b,a], M. Aharrouche[81], S.P. Ahlen[21], F. Ahles[48], A. Ahmad[148], M. Ahsan[40], G. Aielli[133a,133b], T. Akdogan[18a], T.P.A. Åkesson[79], G. Akimoto[155], A.V. Akimov[94], A. Akiyama[67], M.S. Alam[1], M.A. Alam[76], S. Albrand[55], M. Aleksa[29], I.N. Aleksandrov[65], F. Alessandria[89a], C. Alexa[25a], G. Alexander[153], G. Alexandre[49], T. Alexopoulos[9], M. Alhroob[20], M. Aliev[15], G. Alimonti[89a], J. Alison[120], M. Aliyev[10], P.P. Allport[73], S.E. Allwood-Spiers[53], J. Almond[82], A. Aloisio[102a,102b], R. Alon[171], A. Alonso[79], M.G. Alviggi[102a,102b], K. Amako[66], P. Amaral[29], C. Amelung[22], V.V. Ammosov[128], A. Amorim[124a,b], G. Amorós[167], N. Amram[153], C. Anastopoulos[29], N. Andari[115], T. Andeen[34], C.F. Anders[20], K.J. Anderson[30], A. Andreazza[89a,89b], V. Andrei[58a], M-L. Andrieux[55], X.S. Anduaga[70], A. Angerami[34], F. Anghinolfi[29], N. Anjos[124a], A. Annovi[47], A. Antonaki[8], M. Antonelli[47], A. Antonov[96], J. Antos[144b], F. Anulli[132a], S. Aoun[83], L. Aperio Bella[4], R. Apolle[118,c], G. Arabidze[88], I. Aracena[143], Y. Arai[66], A.T.H. Arce[44], J.P. Archambault[28], S. Arfaoui[29,d], J-F. Arguin[14], E. Arik[18a,*], M. Arik[18a], A.J. Armbruster[87], O. Arnaez[81], C. Arnault[115], A. Artamonov[95], G. Artoni[132a,132b], D. Arutinov[20], S. Asai[155], R. Asfandiyarov[172], S. Ask[27], B. Åsman[146a,146b], L. Asquith[5], K. Assamagan[24], A. Astbury[169], A. Astvatsatourov[52], G. Atoian[175], B. Aubert[4], B. Auerbach[175], E. Auge[115], K. Augsten[127], M. Aurousseau[145a], N. Austin[73], R. Avramidou[9], D. Axen[168], C. Ay[54], G. Azuelos[93,e], Y. Azuma[155], M.A. Baak[29], G. Baccaglioni[89a], C. Bacci[134a,134b], A.M. Bach[14], H. Bachacou[136], K. Bachas[29], G. Bachy[29], M. Backes[49], M. Backhaus[20], E. Badescu[25a], P. Bagnaia[132a,132b], S. Bahinipati[2], Y. Bai[32a], D.C. Bailey[158], T. Bain[158], J.T. Baines[129], O.K. Baker[175], M.D. Baker[24], S. Baker[77], F. Baltasar Dos Santos Pedrosa[29], E. Banas[38], P. Banerjee[93], Sw. Banerjee[172], D. Banfi[29], A. Bangert[137], V. Bansal[169], H.S. Bansil[17], L. Barak[171], S.P. Baranov[94], A. Barashkou[65], A. Barbaro Galtieri[14], T. Barber[27], E.L. Barberio[86], D. Barberis[50a,50b], M. Barbero[20], D.Y. Bardin[65], T. Barillari[99], M. Barisonzi[174], T. Barklow[143], N. Barlow[27], B.M. Barnett[129], R.M. Barnett[14], A. Baroncelli[134a], A.J. Barr[118], F. Barreiro[80], J. Barreiro Guimarães da Costa[57], P. Barrillon[115], R. Bartoldus[143], A.E. Barton[71], D. Bartsch[20], V. Bartsch[149], R.L. Bates[53], L. Batkova[144a], J.R. Batley[27], A. Battaglia[16], M. Battistin[29], G. Battistoni[89a], F. Bauer[136], H.S. Bawa[143,f], B. Beare[158], T. Beau[78], P.H. Beauchemin[118], R. Beccherle[50a], P. Bechtle[41], H.P. Beck[16], M. Beckingham[48], K.H. Becks[174], A.J. Beddall[18c], A. Beddall[18c], S. Bedikian[175], V.A. Bednyakov[65], C.P. Bee[83], M. Begel[24], S. Behar Harpaz[152], P.K. Behera[63], M. Beimforde[99], C. Belanger-Champagne[166], P.J. Bell[49], W.H. Bell[49], G. Bella[153], L. Bellagamba[19a], F. Bellina[29], M. Bellomo[119a], A. Belloni[57], O. Beloborodova[107], K. Belotskiy[96], O. Beltramello[29], S. Ben Ami[152], O. Benary[153], D. Benchekroun[135a], C. Benchouk[83], M. Bendel[81], B.H. Benedict[163], N. Benekos[165], Y. Benhammou[153], D.P. Benjamin[44], M. Benoit[115], J.R. Bensinger[22], K. Benslama[130], S. Bentvelsen[105], D. Berge[29], E. Bergeaas Kuutmann[41], N. Berger[4], F. Berghaus[169], E. Berglund[49], J. Beringer[14], K. Bernardet[83], P. Bernat[77], R. Bernhard[48], C. Bernius[24], T. Berry[76], A. Bertin[19a,19b], F. Bertinelli[29], F. Bertolucci[122a,122b], M.I. Besana[89a,89b], N. Besson[136], S. Bethke[99], W. Bhimji[45], R.M. Bianchi[29], M. Bianco[72a,72b], O. Biebel[98], S.P. Bieniek[77], J. Biesiada[14], M. Biglietti[134a,134b], H. Bilokon[47], M. Bindi[19a,19b], S. Binet[115], A. Bingul[18c], C. Bini[132a,132b], C. Biscarat[177], U. Bitenc[48], K.M. Black[21], R.E. Blair[5], J.-B. Blanchard[115], G. Blanchot[29], T. Blazek[144a], C. Blocker[22], J. Blocki[38], A. Blondel[49], W. Blum[81], U. Blumenschein[54], G.J. Bobbink[105], V.B. Bobrovnikov[107], S.S. Bocchetta[79], A. Bocci[44], C.R. Boddy[118], M. Boehler[41], J. Boek[174], N. Boelaert[35], S. Böser[77], J.A. Bogaerts[29], A. Bogdanchikov[107], A. Bogouch[90,*], C. Bohm[146a], V. Boisvert[76], T. Bold[163,g], V. Boldea[25a], N.M. Bolnet[136], M. Bona[75], V.G. Bondarenko[96], M. Boonekamp[136], G. Boorman[76], C.N. Booth[139], S. Bordoni[78], C. Borer[16], A. Borisov[128], G. Borissov[71], I. Borjanovic[12a], S. Borroni[132a,132b], K. Bos[105], D. Boscherini[19a], M. Bosman[11], H. Boterenbrood[105], D. Botterill[129], J. Bouchami[93], J. Boudreau[123], E.V. Bouhova-Thacker[71], C. Boulahouache[123], C. Bourdarios[115], N. Bousson[83], A. Boveia[30], J. Boyd[29], I.R. Boyko[65], N.I. Bozhko[128], I. Bozovic-Jelisavcic[12b], J. Bracinik[17], A. Braem[29], P. Branchini[134a], G.W. Brandenburg[57], A. Brandt[7], G. Brandt[15], O. Brandt[54], U. Bratzler[156], B. Brau[84], J.E. Brau[114], H.M. Braun[174], B. Brelier[158], J. Bremer[29], R. Brenner[166], S. Bressler[152], D. Breton[115], D. Britton[53], F.M. Brochu[27], I. Brock[20], R. Brock[88], T.J. Brodbeck[71], E. Brodet[153], F. Broggi[89a], C. Bromberg[88], G. Brooijmans[34], W.K. Brooks[31b], G. Brown[82], H. Brown[7], P.A. Bruckman de Renstrom[38], D. Bruncko[144b], R. Bruneliere[48], S. Brunet[61], A. Bruni[19a], G. Bruni[19a], M. Bruschi[19a], T. Buanes[13], F. Bucci[49], J. Buchanan[118], N.J. Buchanan[2], P. Buchholz[141], R.M. Buckingham[118], A.G. Buckley[45], S.I. Buda[25a], I.A. Budagov[65], B. Budick[108], V. Büscher[81], L. Bugge[117], D. Buira-Clark[118], O. Bulekov[96], M. Bunse[42], T. Buran[117], H. Burckhart[29], S. Burdin[73], T. Burgess[13], S. Burke[129], E. Busato[33], P. Bussey[53], C.P. Buszello[166], F. Butin[29], B. Butler[143], J.M. Butler[21], C.M. Buttar[53], J.M. Butterworth[77], W. Buttinger[27], T. Byatt[77], S. Cabrera Urbán[167], D. Caforio[19a,19b], O. Cakir[3a], P. Calafiura[14], G. Calderini[78], P. Calfayan[98], R. Calkins[106], L.P. Caloba[23a], R. Caloi[132a,132b],

D. Calvet[33], S. Calvet[33], R. Camacho Toro[33], P. Camarri[133a,133b], M. Cambiaghi[119a,119b], D. Cameron[117], S. Campana[29], M. Campanelli[77], V. Canale[102a,102b], F. Canelli[30], A. Canepa[159a], J. Cantero[80], L. Capasso[102a,102b], M.D.M. Capeans Garrido[29], I. Caprini[25a], M. Caprini[25a], D. Capriotti[99], M. Capua[36a,36b], R. Caputo[148], C. Caramarcu[25a], R. Cardarelli[133a], T. Carli[29], G. Carlino[102a], L. Carminati[89a,89b], B. Caron[159a], S. Caron[48], G.D. Carrillo Montoya[172], A.A. Carter[75], J.R. Carter[27], J. Carvalho[124a,h], D. Casadei[108], M.P. Casado[11], M. Cascella[122a,122b], C. Caso[50a,50b,*], A.M. Castaneda Hernandez[172], E. Castaneda-Miranda[172], V. Castillo Gimenez[167], N.F. Castro[124a], G. Cataldi[72a], F. Cataneo[29], A. Catinaccio[29], J.R. Catmore[71], A. Cattai[29], G. Cattani[133a,133b], S. Caughron[88], D. Cauz[164a,164c], P. Cavalleri[78], D. Cavalli[89a], M. Cavalli-Sforza[11], V. Cavasinni[122a,122b], F. Ceradini[134a,134b], A.S. Cerqueira[23a], A. Cerri[29], L. Cerrito[75], F. Cerutti[47], S.A. Cetin[18b], F. Cevenini[102a,102b], A. Chafaq[135a], D. Chakraborty[106], K. Chan[2], B. Chapleau[85], J.D. Chapman[27], J.W. Chapman[87], E. Chareyre[78], D.G. Charlton[17], V. Chavda[82], C.A. Chavez Barajas[29], S. Cheatham[85], S. Chekanov[5], S.V. Chekulaev[159a], G.A. Chelkov[65], M.A. Chelstowska[104], C. Chen[64], H. Chen[24], S. Chen[32c], T. Chen[32c], X. Chen[172], S. Cheng[32a], A. Cheplakov[65], V.F. Chepurnov[65], R. Cherkaoui El Moursli[135e], V. Chernyatin[24], E. Cheu[6], S.L. Cheung[158], L. Chevalier[136], G. Chiefari[102a,102b], L. Chikovani[51], J.T. Childers[58a], A. Chilingarov[71], G. Chiodini[72a], M.V. Chizhov[65], G. Choudalakis[30], S. Chouridou[137], I.A. Christidi[77], A. Christov[48], D. Chromek-Burckhart[29], M.L. Chu[151], J. Chudoba[125], G. Ciapetti[132a,132b], K. Ciba[37], A.K. Ciftci[3a], R. Ciftci[3a], D. Cinca[33], V. Cindro[74], M.D. Ciobotaru[163], C. Ciocca[19a,19b], A. Ciocio[14], M. Cirilli[87], M. Ciubancan[25a], A. Clark[49], P.J. Clark[45], W. Cleland[123], J.C. Clemens[83], B. Clement[55], C. Clement[146a,146b], R.W. Clifft[129], Y. Coadou[83], M. Cobal[164a,164c], A. Coccaro[50a,50b], J. Cochran[64], P. Coe[118], J.G. Cogan[143], J. Coggeshall[165], E. Cogneras[177], C.D. Cojocaru[28], J. Colas[4], A.P. Colijn[105], C. Collard[115], N.J. Collins[17], C. Collins-Tooth[53], J. Collot[55], G. Colon[84], P. Conde Muiño[124a], E. Coniavitis[118], M.C. Conidi[11], M. Consonni[104], V. Consorti[48], S. Constantinescu[25a], C. Conta[119a,119b], F. Conventi[102a,i], J. Cook[29], M. Cooke[14], B.D. Cooper[77], A.M. Cooper-Sarkar[118], N.J. Cooper-Smith[76], K. Copic[34], T. Cornelissen[50a,50b], M. Corradi[19a], F. Corriveau[85,j], A. Cortes-Gonzalez[165], G. Cortiana[99], G. Costa[89a], M.J. Costa[167], D. Costanzo[139], T. Costin[30], D. Côté[29], R. Coura Torres[23a], L. Courneyea[169], G. Cowan[76], C. Cowden[27], B.E. Cox[82], K. Cranmer[108], F. Crescioli[122a,122b], M. Cristinziani[20], G. Crosetti[36a,36b], R. Crupi[72a,72b], S. Crépé-Renaudin[55], C.-M. Cuciuc[25a], C. Cuenca Almenar[175], T. Cuhadar Donszelmann[139], S. Cuneo[50a,50b], M. Curatolo[47], C.J. Curtis[17], P. Cwetanski[61], H. Czirr[141], Z. Czyczula[117], S. D'Auria[53], M. D'Onofrio[73], A. D'Orazio[132a,132b], P.V.M. Da Silva[23a], C. Da Via[82], W. Dabrowski[37], T. Dai[87], C. Dallapiccola[84], M. Dam[35], M. Dameri[50a,50b], D.S. Damiani[137], H.O. Danielsson[29], D. Dannheim[99], V. Dao[49], G. Darbo[50a], G.L. Darlea[25b], C. Daum[105], J.P. Dauvergne[29], W. Davey[86], T. Davidek[126], N. Davidson[86], R. Davidson[71], E. Davies[118,c], M. Davies[93], A.R. Davison[77], Y. Davygora[58a], E. Dawe[142], I. Dawson[139], J.W. Dawson[5,*], R.K. Daya[39], K. De[7], R. de Asmundis[102a], S. De Castro[19a,19b], P.E. De Castro Faria Salgado[24], S. De Cecco[78], J. de Graat[98], N. De Groot[104], P. de Jong[105], C. De La Taille[115], H. De la Torre[80], B. De Lotto[164a,164c], L. De Mora[71], L. De Nooij[105], M. De Oliveira Branco[29], D. De Pedis[132a], P. de Saintignon[55], A. De Salvo[132a], U. De Sanctis[164a,164c], A. De Santo[149], J.B. De Vivie De Regie[115], S. Dean[77], D.V. Dedovich[65], J. Degenhardt[120], M. Dehchar[118], M. Deile[98], C. Del Papa[164a,164c], J. Del Peso[80], T. Del Prete[122a,122b], M. Deliyergiyev[74], A. Dell'Acqua[29], L. Dell'Asta[89a,89b], M. Della Pietra[102a,i], D. della Volpe[102a,102b], M. Delmastro[29], P. Delpierre[83], N. Delruelle[29], P.A. Delsart[55], C. Deluca[148], S. Demers[175], M. Demichev[65], B. Demirkoz[11,k], J. Deng[163], S.P. Denisov[128], D. Derendarz[38], J.E. Derkaoui[135d], F. Derue[78], P. Dervan[73], K. Desch[20], E. Devetak[148], P.O. Deviveiros[158], A. Dewhurst[129], B. DeWilde[148], S. Dhaliwal[158], R. Dhullipudi[24,l], A. Di Ciaccio[133a,133b], L. Di Ciaccio[4], A. Di Girolamo[29], B. Di Girolamo[29], S. Di Luise[134a,134b], A. Di Mattia[88], B. Di Micco[29], R. Di Nardo[133a,133b], A. Di Simone[133a,133b], R. Di Sipio[19a,19b], M.A. Diaz[31a], F. Diblen[18c], E.B. Diehl[87], J. Dietrich[41], T.A. Dietzsch[58a], S. Diglio[115], K. Dindar Yagci[39], J. Dingfelder[20], C. Dionisi[132a,132b], P. Dita[25a], S. Dita[25a], F. Dittus[29], F. Djama[83], T. Djobava[51], M.A.B. do Vale[23a], A. Do Valle Wemans[124a], T.K.O. Doan[4], M. Dobbs[85], R. Dobinson[29,*], D. Dobos[42], E. Dobson[29], M. Dobson[163], J. Dodd[34], C. Doglioni[118], T. Doherty[53], Y. Doi[66,*], J. Dolejsi[126], I. Dolenc[74], Z. Dolezal[126], B.A. Dolgoshein[96,*], T. Dohmae[155], M. Donadelli[23b], M. Donega[120], J. Donini[55], J. Dopke[29], A. Doria[102a], A. Dos Anjos[172], M. Dosil[11], A. Dotti[122a,122b], M.T. Dova[70], J.D. Dowell[17], A.D. Doxiadis[105], A.T. Doyle[53], Z. Drasal[126], J. Drees[174], N. Dressnandt[120], H. Drevermann[29], C. Driouichi[35], M. Dris[9], J. Dubbert[99], T. Dubbs[137], S. Dube[14], E. Duchovni[171], G. Duckeck[98], A. Dudarev[29], F. Dudziak[64], M. Dührssen[29], I.P. Duerdoth[82], L. Duflot[115], M-A. Dufour[85], M. Dunford[29], H. Duran Yildiz[3b], R. Duxfield[139], M. Dwuznik[37], F. Dydak[29], D. Dzahini[55], M. Düren[52], W.L. Ebenstein[44], J. Ebke[98], S. Eckert[48], S. Eckweiler[81], K. Edmonds[81], C.A. Edwards[76], N.C. Edwards[53], W. Ehrenfeld[41], T. Ehrich[99], T. Eifert[29], G. Eigen[13], K. Einsweiler[14], E. Eisenhandler[75], T. Ekelof[166], M. El Kacimi[135c], M. Ellert[166], S. Elles[4], F. Ellinghaus[81], K. Ellis[75], N. Ellis[29], J. Elmsheuser[98], M. Elsing[29], R. Ely[14], D. Emeliyanov[129], R. Engelmann[148], A. Engl[98], B. Epp[62], A. Eppig[87], J. Erdmann[54], A. Ereditato[16], D. Eriksson[146a], J. Ernst[1], M. Ernst[24], J. Ernwein[136], D. Errede[165], S. Errede[165], E. Ertel[81], M. Escalier[115], C. Escobar[167], X. Espinal Curull[11], B. Esposito[47], F. Etienne[83], A.I. Etienvre[136], E. Etzion[153], D. Evangelakou[54], H. Evans[61], L. Fabbri[19a,19b], C. Fabre[29], R.M. Fakhrutdinov[128], S. Falciano[132a], A.C. Falou[115], Y. Fang[172], M. Fanti[89a,89b], A. Farbin[7], A. Farilla[134a], J. Farley[148], T. Farooque[158], S.M. Farrington[118], P. Farthouat[29], P. Fassnacht[29], D. Fassouliotis[8], B. Fatholahzadeh[158], A. Favareto[89a,89b], L. Fayard[115], S. Fazio[36a,36b],

R. Febbraro[33], P. Federic[144a], O.L. Fedin[121], W. Fedorko[88], M. Fehling-Kaschek[48], L. Feligioni[83], D. Fellmann[5], C.U. Felzmann[86], C. Feng[32d], E.J. Feng[30], A.B. Fenyuk[128], J. Ferencei[144b], J. Ferland[93], W. Fernando[109], S. Ferrag[53], J. Ferrando[53], V. Ferrara[41], A. Ferrari[166], P. Ferrari[105], R. Ferrari[119a], A. Ferrer[167], M.L. Ferrer[47], D. Ferrere[49], C. Ferretti[87], A. Ferretto Parodi[50a,50b], M. Fiascaris[30], F. Fiedler[81], A. Filipčič[74], A. Filippas[9], F. Filthaut[104], M. Fincke-Keeler[169], M.C.N. Fiolhais[124a,h], L. Fiorini[167], A. Firan[39], G. Fischer[41], P. Fischer[20], M.J. Fisher[109], S.M. Fisher[129], M. Flechl[48], I. Fleck[141], J. Fleckner[81], P. Fleischmann[173], S. Fleischmann[174], T. Flick[174], L.R. Flores Castillo[172], M.J. Flowerdew[99], F. Föhlisch[58a], M. Fokitis[9], T. Fonseca Martin[16], D.A. Forbush[138], A. Formica[136], A. Forti[82], D. Fortin[159a], J.M. Foster[82], D. Fournier[115], A. Foussat[29], A.J. Fowler[44], K. Fowler[137], H. Fox[71], P. Francavilla[122a,122b], S. Franchino[119a,119b], D. Francis[29], T. Frank[171], M. Franklin[57], S. Franz[29], M. Fraternali[119a,119b], S. Fratina[120], S.T. French[27], R. Froeschl[29], D. Froidevaux[29], J.A. Frost[27], C. Fukunaga[156], E. Fullana Torregrosa[29], J. Fuster[167], C. Gabaldon[29], O. Gabizon[171], T. Gadfort[24], S. Gadomski[49], G. Gagliardi[50a,50b], P. Gagnon[61], C. Galea[98], E.J. Gallas[118], M.V. Gallas[29], V. Gallo[16], B.J. Gallop[129], P. Gallus[125], E. Galyaev[40], K.K. Gan[109], Y.S. Gao[143,f], V.A. Gapienko[128], A. Gaponenko[14], F. Garberson[175], M. Garcia-Sciveres[14], C. García[167], J.E. García Navarro[49], R.W. Gardner[30], N. Garelli[29], H. Garitaonandia[105], V. Garonne[29], J. Garvey[17], C. Gatti[47], G. Gaudio[119a], O. Gaumer[49], B. Gaur[141], L. Gauthier[136], I.L. Gavrilenko[94], C. Gay[168], G. Gaycken[20], J-C. Gayde[29], E.N. Gazis[9], P. Ge[32d], C.N.P. Gee[129], D.A.A. Geerts[105], Ch. Geich-Gimbel[20], K. Gellerstedt[146a,146b], C. Gemme[50a], A. Gemmell[53], M.H. Genest[98], S. Gentile[132a,132b], M. George[54], S. George[76], P. Gerlach[174], A. Gershon[153], C. Geweniger[58a], H. Ghazlane[135b], P. Ghez[4], N. Ghodbane[33], B. Giacobbe[19a], S. Giagu[132a,132b], V. Giakoumopoulou[8], V. Giangiobbe[122a,122b], F. Gianotti[29], B. Gibbard[24], A. Gibson[158], S.M. Gibson[29], L.M. Gilbert[118], M. Gilchriese[14], V. Gilewsky[91], D. Gillberg[28], A.R. Gillman[129], D.M. Gingrich[2,e], J. Ginzburg[153], N. Giokaris[8], R. Giordano[102a,102b], F.M. Giorgi[15], P. Giovannini[99], P.F. Giraud[136], D. Giugni[89a], M. Giunta[132a,132b], P. Giusti[19a], B.K. Gjelsten[117], L.K. Gladilin[97], C. Glasman[80], J. Glatzer[48], A. Glazov[41], K.W. Glitza[174], G.L. Glonti[65], J. Godfrey[142], J. Godlewski[29], M. Goebel[41], T. Göpfert[43], C. Goeringer[81], C. Gössling[42], T. Göttfert[99], S. Goldfarb[87], D. Goldin[39], T. Golling[175], S.N. Golovnia[128], A. Gomes[124a,b], L.S. Gomez Fajardo[41], R. Gonçalo[76], J. Goncalves Pinto Firmino Da Costa[41], L. Gonella[20], A. Gonidec[29], S. Gonzalez[172], S. González de la Hoz[167], M.L. Gonzalez Silva[26], S. Gonzalez-Sevilla[49], J.J. Goodson[148], L. Goossens[29], P.A. Gorbounov[95], H.A. Gordon[24], I. Gorelov[103], G. Gorfine[174], B. Gorini[29], E. Gorini[72a,72b], A. Gorišek[74], E. Gornicki[38], S.A. Gorokhov[128], V.N. Goryachev[128], B. Gosdzik[41], M. Gosselink[105], M.I. Gostkin[65], M. Gouanère[4], I. Gough Eschrich[163], M. Gouighri[135a], D. Goujdami[135c], M.P. Goulette[49], A.G. Goussiou[138], C. Goy[4], I. Grabowska-Bold[163,g], V. Grabski[176], P. Grafström[29], C. Grah[174], K-J. Grahn[41], F. Grancagnolo[72a], S. Grancagnolo[15], V. Grassi[148], V. Gratchev[121], N. Grau[34], H.M. Gray[29], J.A. Gray[148], E. Graziani[134a], O.G. Grebenyuk[121], D. Greenfield[129], T. Greenshaw[73], Z.D. Greenwood[24,l], I.M. Gregor[41], P. Grenier[143], J. Griffiths[138], N. Grigalashvili[65], A.A. Grillo[137], S. Grinstein[11], Y.V. Grishkevich[97], J.-F. Grivaz[115], J. Grognuz[29], M. Groh[99], E. Gross[171], J. Grosse-Knetter[54], J. Groth-Jensen[171], K. Grybel[141], V.J. Guarino[5], D. Guest[175], C. Guicheney[33], A. Guida[72a,72b], T. Guillemin[4], S. Guindon[54], H. Guler[85,m], J. Gunther[125], B. Guo[158], J. Guo[34], A. Gupta[30], Y. Gusakov[65], V.N. Gushchin[128], A. Gutierrez[93], P. Gutierrez[111], N. Guttman[153], O. Gutzwiller[172], C. Guyot[136], C. Gwenlan[118], C.B. Gwilliam[73], A. Haas[143], S. Haas[29], C. Haber[14], R. Hackenburg[24], H.K. Hadavand[39], D.R. Hadley[17], P. Haefner[99], F. Hahn[29], S. Haider[29], Z. Hajduk[38], H. Hakobyan[176], J. Haller[54], K. Hamacher[174], P. Hamal[113], A. Hamilton[49], S. Hamilton[161], H. Han[32a], L. Han[32b], K. Hanagaki[116], M. Hance[120], C. Handel[81], P. Hanke[58a], J.R. Hansen[35], J.B. Hansen[35], J.D. Hansen[35], P.H. Hansen[35], P. Hansson[143], K. Hara[160], G.A. Hare[137], T. Harenberg[174], S. Harkusha[90], D. Harper[87], R.D. Harrington[21], O.M. Harris[138], K. Harrison[17], J. Hartert[48], F. Hartjes[105], T. Haruyama[66], A. Harvey[56], S. Hasegawa[101], Y. Hasegawa[140], S. Hassani[136], M. Hatch[29], D. Hauff[99], S. Haug[16], M. Hauschild[29], R. Hauser[88], M. Havranek[20], B.M. Hawes[118], C.M. Hawkes[17], R.J. Hawkings[29], D. Hawkins[163], T. Hayakawa[67], D. Hayden[76], H.S. Hayward[73], S.J. Haywood[129], E. Hazen[21], M. He[32d], S.J. Head[17], V. Hedberg[79], L. Heelan[7], S. Heim[88], B. Heinemann[14], S. Heisterkamp[35], L. Helary[4], M. Heller[115], S. Hellman[146a,146b], C. Helsens[11], R.C.W. Henderson[71], M. Henke[58a], A. Henrichs[54], A.M. Henriques Correia[29], S. Henrot-Versille[115], F. Henry-Couannier[83], C. Hensel[54], T. Henß[174], C.M. Hernandez[7], Y. Hernández Jiménez[167], R. Herrberg[15], A.D. Hershenhorn[152], G. Herten[48], R. Hertenberger[98], L. Hervas[29], N.P. Hessey[105], A. Hidvegi[146a], E. Higón-Rodriguez[167], D. Hill[5,*], J.C. Hill[27], N. Hill[5], K.H. Hiller[41], S. Hillert[20], S.J. Hillier[17], I. Hinchliffe[14], E. Hines[120], M. Hirose[116], F. Hirsch[42], D. Hirschbuehl[174], J. Hobbs[148], N. Hod[153], M.C. Hodgkinson[139], P. Hodgson[139], A. Hoecker[29], M.R. Hoeferkamp[103], J. Hoffman[39], D. Hoffmann[83], M. Hohlfeld[81], M. Holder[141], A. Holmes[118], S.O. Holmgren[146a], T. Holy[127], J.L. Holzbauer[88], Y. Homma[67], T.M. Hong[120], L. Hooft van Huysduynen[108], T. Horazdovsky[127], C. Horn[143], S. Horner[48], K. Horton[118], J-Y. Hostachy[55], S. Hou[151], M.A. Houlden[73], A. Hoummada[135a], J. Howarth[82], D.F. Howell[118], I. Hristova[41], J. Hrivnac[115], I. Hruska[125], T. Hryn'ova[4], P.J. Hsu[175], S.-C. Hsu[14], G.S. Huang[111], Z. Hubacek[127], F. Hubaut[83], F. Huegging[20], T.B. Huffman[118], E.W. Hughes[34], G. Hughes[71], R.E. Hughes-Jones[82], M. Huhtinen[29], P. Hurst[57], M. Hurwitz[14], U. Husemann[41], N. Huseynov[65,n], J. Huston[88], J. Huth[57], G. Iacobucci[49], G. Iakovidis[9], M. Ibbotson[82], I. Ibragimov[141], R. Ichimiya[67], L. Iconomidou-Fayard[115], J. Idarraga[115],

M. Idzik[37], P. Iengo[102a,102b], O. Igonkina[105], Y. Ikegami[66], M. Ikeno[66], Y. Ilchenko[39], D. Iliadis[154], D. Imbault[78], M. Imhaeuser[174], M. Imori[155], T. Ince[20], J. Inigo-Golfin[29], P. Ioannou[8], M. Iodice[134a], G. Ionescu[4], A. Irles Quiles[167], K. Ishii[66], A. Ishikawa[67], M. Ishino[66], R. Ishmukhametov[39], C. Issever[118], S. Istin[18a], Y. Itoh[101], A.V. Ivashin[128], W. Iwanski[38], H. Iwasaki[66], J.M. Izen[40], V. Izzo[102a], B. Jackson[120], J.N. Jackson[73], P. Jackson[143], M.R. Jaekel[29], V. Jain[61], K. Jakobs[48], S. Jakobsen[35], J. Jakubek[127], D.K. Jana[111], E. Jankowski[158], E. Jansen[77], A. Jantsch[99], M. Janus[20], G. Jarlskog[79], L. Jeanty[57], K. Jelen[37], I. Jen-La Plante[30], P. Jenni[29], A. Jeremie[4], P. Jež[35], S. Jézéquel[4], M.K. Jha[19a], H. Ji[172], W. Ji[81], J. Jia[148], Y. Jiang[32b], M. Jimenez Belenguer[41], G. Jin[32b], S. Jin[32a], O. Jinnouchi[157], M.D. Joergensen[35], D. Joffe[39], L.G. Johansen[13], M. Johansen[146a,146b], K.E. Johansson[146a], P. Johansson[139], S. Johnert[41], K.A. Johns[6], K. Jon-And[146a,146b], G. Jones[82], R.W.L. Jones[71], T.W. Jones[77], T.J. Jones[73], O. Jonsson[29], C. Joram[29], P.M. Jorge[124a,b], J. Joseph[14], T. Jovin[12b], X. Ju[130], V. Juranek[125], P. Jussel[62], V.V. Kabachenko[128], S. Kabana[16], M. Kaci[167], A. Kaczmarska[38], P. Kadlecik[35], M. Kado[115], H. Kagan[109], M. Kagan[57], S. Kaiser[99], E. Kajomovitz[152], S. Kalinin[174], L.V. Kalinovskaya[65], S. Kama[39], N. Kanaya[155], M. Kaneda[29], T. Kanno[157], V.A. Kantserov[96], J. Kanzaki[66], B. Kaplan[175], A. Kapliy[30], J. Kaplon[29], D. Kar[43], M. Karagoz[118], M. Karnevskiy[41], K. Karr[5], V. Kartvelishvili[71], A.N. Karyukhin[128], L. Kashif[172], A. Kasmi[39], R.D. Kass[109], A. Kastanas[13], M. Kataoka[4], Y. Kataoka[155], E. Katsoufis[9], J. Katzy[41], V. Kaushik[6], K. Kawagoe[67], T. Kawamoto[155], G. Kawamura[81], M.S. Kayl[105], V.A. Kazanin[107], M.Y. Kazarinov[65], J.R. Keates[82], R. Keeler[169], R. Kehoe[39], M. Keil[54], G.D. Kekelidze[65], M. Kelly[82], J. Kennedy[98], C.J. Kenney[143], M. Kenyon[53], O. Kepka[125], N. Kerschen[29], B.P. Kerševan[74], S. Kersten[174], K. Kessoku[155], C. Ketterer[48], J. Keung[158], M. Khakzad[28], F. Khalil-zada[10], H. Khandanyan[165], A. Khanov[112], D. Kharchenko[65], A. Khodinov[96], A.G. Kholodenko[128], A. Khomich[58a], T.J. Khoo[27], G. Khoriauli[20], A. Khoroshilov[174], N. Khovanskiy[65], V. Khovanskiy[95], E. Khramov[65], J. Khubua[51], H. Kim[7], M.S. Kim[2], P.C. Kim[143], S.H. Kim[160], N. Kimura[170], O. Kind[15], B.T. King[73], M. King[67], R.S.B. King[118], J. Kirk[129], G.P. Kirsch[118], L.E. Kirsch[22], A.E. Kiryunin[99], D. Kisielewska[37], T. Kittelmann[123], A.M. Kiver[128], H. Kiyamura[67], E. Kladiva[144b], J. Klaiber-Lodewigs[42], M. Klein[73], U. Klein[73], K. Kleinknecht[81], M. Klemetti[85], A. Klier[171], A. Klimentov[24], R. Klingenberg[42], E.B. Klinkby[35], T. Klioutchnikova[29], P.F. Klok[104], S. Klous[105], E.-E. Kluge[58a], T. Kluge[73], P. Kluit[105], S. Kluth[99], E. Kneringer[62], J. Knobloch[29], E.B.F.G. Knoops[83], A. Knue[54], B.R. Ko[44], T. Kobayashi[155], M. Kobel[43], M. Kocian[143], A. Kocnar[113], P. Kodys[126], K. Köneke[29], A.C. König[104], S. Koenig[81], L. Köpke[81], F. Koetsveld[104], P. Koevesarki[20], T. Koffas[29], E. Koffeman[105], F. Kohn[54], Z. Kohout[127], T. Kohriki[66], T. Koi[143], T. Kokott[20], G.M. Kolachev[107], H. Kolanoski[15], V. Kolesnikov[65], I. Koletsou[89a], J. Koll[88], D. Kollar[29], M. Kollefrath[48], S.D. Kolya[82], A.A. Komar[94], J.R. Komaragiri[142], Y. Komori[155], T. Kondo[66], T. Kono[41,o], A.I. Kononov[48], R. Konoplich[108,p], N. Konstantinidis[77], A. Kootz[174], S. Koperny[37], S.V. Kopikov[128], K. Korcyl[38], K. Kordas[154], V. Koreshev[128], A. Korn[14], A. Korol[107], I. Korolkov[11], E.V. Korolkova[139], V.A. Korotkov[128], O. Kortner[99], S. Kortner[99], V.V. Kostyukhin[20], M.J. Kotamäki[29], S. Kotov[99], V.M. Kotov[65], A. Kotwal[44], C. Kourkoumelis[8], V. Kouskoura[154], A. Koutsman[105], R. Kowalewski[169], T.Z. Kowalski[37], W. Kozanecki[136], A.S. Kozhin[128], V. Kral[127], V.A. Kramarenko[97], G. Kramberger[74], O. Krasel[42], M.W. Krasny[78], A. Krasznahorkay[108], J. Kraus[88], A. Kreisel[153], F. Krejci[127], J. Kretzschmar[73], N. Krieger[54], P. Krieger[158], K. Kroeninger[54], H. Kroha[99], J. Kroll[120], J. Kroseberg[20], J. Krstic[12a], U. Kruchonak[65], H. Krüger[20], T. Kruker[16], Z.V. Krumshteyn[65], A. Kruth[20], T. Kubota[86], S. Kuehn[48], A. Kugel[58c], T. Kuhl[174], D. Kuhn[62], V. Kukhtin[65], Y. Kulchitsky[90], S. Kuleshov[31b], C. Kummer[98], M. Kuna[78], N. Kundu[118], J. Kunkle[120], A. Kupco[125], H. Kurashige[67], M. Kurata[160], Y.A. Kurochkin[90], V. Kus[125], W. Kuykendall[138], M. Kuze[157], P. Kuzhir[91], O. Kvasnicka[125], J. Kvita[29], R. Kwee[15], A. La Rosa[172], L. La Rotonda[36a,36b], L. Labarga[80], J. Labbe[4], S. Lablak[135a], C. Lacasta[167], F. Lacava[132a,132b], H. Lacker[15], D. Lacour[78], V.R. Lacuesta[167], E. Ladygin[65], R. Lafaye[4], B. Laforge[78], T. Lagouri[80], S. Lai[48], E. Laisne[55], M. Lamanna[29], C.L. Lampen[6], W. Lampl[6], E. Lancon[136], U. Landgraf[48], M.P.J. Landon[75], H. Landsman[152], J.L. Lane[82], C. Lange[41], A.J. Lankford[163], F. Lanni[24], K. Lantzsch[29], S. Laplace[78], C. Lapoire[20], J.F. Laporte[136], T. Lari[89a], A.V. Larionov[128], A. Larner[118], C. Lasseur[29], M. Lassnig[29], W. Lau[118], P. Laurelli[47], A. Lavorato[118], W. Lavrijsen[14], P. Laycock[73], A.B. Lazarev[65], A. Lazzaro[89a,89b], O. Le Dortz[78], E. Le Guirriec[83], C. Le Maner[158], E. Le Menedeu[136], C. Lebel[93], T. LeCompte[5], F. Ledroit-Guillon[55], H. Lee[105], J.S.H. Lee[150], S.C. Lee[151], L. Lee[175], M. Lefebvre[169], M. Legendre[136], A. Leger[49], B.C. LeGeyt[120], F. Legger[98], C. Leggett[14], M. Lehmacher[20], G. Lehmann Miotto[29], X. Lei[6], M.A.L. Leite[23b], R. Leitner[126], D. Lellouch[171], J. Lellouch[78], M. Leltchouk[34], V. Lendermann[58a], K.J.C. Leney[145b], T. Lenz[174], G. Lenzen[174], B. Lenzi[29], K. Leonhardt[43], S. Leontsinis[9], C. Leroy[93], J-R. Lessard[169], J. Lesser[146a], C.G. Lester[27], A. Leung Fook Cheong[172], J. Levêque[4], D. Levin[87], L.J. Levinson[171], M.S. Levitski[128], M. Lewandowska[21], A. Lewis[118], G.H. Lewis[108], A.M. Leyko[20], M. Leyton[15], B. Li[83], H. Li[172], S. Li[32b,d], X. Li[87], Z. Liang[39], Z. Liang[118,q], B. Liberti[133a], P. Lichard[29], M. Lichtnecker[98], K. Lie[165], W. Liebig[13], R. Lifshitz[152], J.N. Lilley[17], C. Limbach[20], A. Limosani[86], M. Limper[63], S.C. Lin[151,r], F. Linde[105], J.T. Linnemann[88], E. Lipeles[120], L. Lipinsky[125], A. Lipniacka[13], T.M. Liss[165], D. Lissauer[24], A. Lister[49], A.M. Litke[137], C. Liu[28], D. Liu[151,s], H. Liu[87], J.B. Liu[87], M. Liu[32b], S. Liu[2], Y. Liu[32b], M. Livan[119a,119b], S.S.A. Livermore[118], A. Lleres[55], J. Llorente Merino[80], S.L. Lloyd[75], E. Lobodzinska[41], P. Loch[6], W.S. Lockman[137], S. Lockwitz[175], T. Loddenkoetter[20], F.K. Loebinger[82], A. Loginov[175], C.W. Loh[168], T. Lohse[15],

K. Lohwasser[48], M. Lokajicek[125], J. Loken[118], V.P. Lombardo[4], R.E. Long[71], L. Lopes[124a,b], D. Lopez Mateos[34,t], M. Losada[162], P. Loscutoff[14], F. Lo Sterzo[132a,132b], M.J. Losty[159a], X. Lou[40], A. Lounis[115], K.F. Loureiro[162], J. Love[21], P.A. Love[71], A.J. Lowe[143,f], F. Lu[32a], H.J. Lubatti[138], C. Luci[132a,132b], A. Lucotte[55], A. Ludwig[43], D. Ludwig[41], I. Ludwig[48], J. Ludwig[48], F. Luehring[61], G. Luijckx[105], D. Lumb[48], L. Luminari[132a], E. Lund[117], B. Lund-Jensen[147], B. Lundberg[79], J. Lundberg[146a,146b], J. Lundquist[35], M. Lungwitz[81], A. Lupi[122a,122b], G. Lutz[99], D. Lynn[24], J. Lys[14], E. Lytken[79], H. Ma[24], L.L. Ma[172], J.A. Macana Goia[93], G. Maccarrone[47], A. Macchiolo[99], B. Maček[74], J. Machado Miguens[124a], D. Macina[49], R. Mackeprang[35], R.J. Madaras[14], W.F. Mader[43], R. Maenner[58c], T. Maeno[24], P. Mättig[174], S. Mättig[41], P.J. Magalhaes Martins[124a,h], L. Magnoni[29], E. Magradze[54], Y. Mahalalel[153], K. Mahboubi[48], G. Mahout[17], C. Maiani[132a,132b], C. Maidantchik[23a], A. Maio[124a,b], S. Majewski[24], Y. Makida[66], N. Makovec[115], P. Mal[6], Pa. Malecki[38], P. Malecki[38], V.P. Maleev[121], F. Malek[55], U. Mallik[63], D. Malon[5], S. Maltezos[9], V. Malyshev[107], S. Malyukov[29], R. Mameghani[98], J. Mamuzic[12b], A. Manabe[66], L. Mandelli[89a], I. Mandić[74], R. Mandrysch[15], J. Maneira[124a], P.S. Mangeard[88], I.D. Manjavidze[65], A. Mann[54], P.M. Manning[137], A. Manousakis-Katsikakis[8], B. Mansoulie[136], A. Manz[99], A. Mapelli[29], L. Mapelli[29], L. March[80], J.F. Marchand[29], F. Marchese[133a,133b], G. Marchiori[78], M. Marcisovsky[125], A. Marin[21,*], C.P. Marino[61], F. Marroquim[23a], R. Marshall[82], Z. Marshall[29], F.K. Martens[158], S. Marti-Garcia[167], A.J. Martin[175], B. Martin[29], B. Martin[88], F.F. Martin[120], J.P. Martin[93], Ph. Martin[55], T.A. Martin[17], B. Martin dit Latour[49], M. Martinez[11], V. Martinez Outschoorn[57], A.C. Martyniuk[82], M. Marx[82], F. Marzano[132a], A. Marzin[111], L. Masetti[81], T. Mashimo[155], R. Mashinistov[94], J. Masik[82], A.L. Maslennikov[107], M. Maß[42], I. Massa[19a,19b], G. Massaro[105], N. Massol[4], P. Mastrandrea[132a,132b], A. Mastroberardino[36a,36b], T. Masubuchi[155], M. Mathes[20], P. Matricon[115], H. Matsumoto[155], H. Matsunaga[155], T. Matsushita[67], C. Mattravers[118,c], J.M. Maugain[29], S.J. Maxfield[73], D.A. Maximov[107], E.N. May[5], A. Mayne[139], R. Mazini[151], M. Mazur[20], M. Mazzanti[89a], E. Mazzoni[122a,122b], S.P. Mc Kee[87], A. McCarn[165], R.L. McCarthy[148], T.G. McCarthy[28], N.A. McCubbin[129], K.W. McFarlane[56], J.A. Mcfayden[139], H. McGlone[53], G. Mchedlidze[51], R.A. McLaren[29], T. Mclaughlan[17], S.J. McMahon[129], R.A. McPherson[169,j], A. Meade[84], J. Mechnich[105], M. Mechtel[174], M. Medinnis[41], R. Meera-Lebbai[111], T. Meguro[116], R. Mehdiyev[93], S. Mehlhase[35], A. Mehta[73], K. Meier[58a], J. Meinhardt[48], B. Meirose[79], C. Melachrinos[30], B.R. Mellado Garcia[172], L. Mendoza Navas[162], Z. Meng[151,s], A. Mengarelli[19a,19b], S. Menke[99], C. Menot[29], E. Meoni[11], K.M. Mercurio[57], P. Mermod[118], L. Merola[102a,102b], C. Meroni[89a], F.S. Merritt[30], A. Messina[29], J. Metcalfe[103], A.S. Mete[64], S. Meuser[20], C. Meyer[81], J-P. Meyer[136], J. Meyer[173], J. Meyer[54], T.C. Meyer[29], W.T. Meyer[64], J. Miao[32d], S. Michal[29], L. Micu[25a], R.P. Middleton[129], P. Miele[29], S. Migas[73], L. Mijović[41], G. Mikenberg[171], M. Mikestikova[125], M. Mikuž[74], D.W. Miller[143], R.J. Miller[88], W.J. Mills[168], C. Mills[57], A. Milov[171], D.A. Milstead[146a,146b], D. Milstein[171], A.A. Minaenko[128], M. Miñano[167], I.A. Minashvili[65], A.I. Mincer[108], B. Mindur[37], M. Mineev[65], Y. Ming[130], A.S. Minot[115], L.M. Mir[11], G. Mirabelli[132a], L. Miralles Verge[11], A. Misiejuk[76], J. Mitrevski[137], G.Y. Mitrofanov[128], V.A. Mitsou[167], S. Mitsui[66], P.S. Miyagawa[82], K. Miyazaki[67], J.U. Mjörnmark[79], T. Moa[146a,146b], P. Mockett[138], S. Moed[57], V. Moeller[27], K. Mönig[41], N. Möser[20], S. Mohapatra[148], B. Mohn[13], W. Mohr[48], S. Mohrdieck-Möck[99], A.M. Moisseev[128,*], R. Moles-Valls[167], J. Molina-Perez[29], J. Monk[77], E. Monnier[83], S. Montesano[89a,89b], F. Monticelli[70], S. Monzani[19a,19b], R.W. Moore[2], G.F. Moorhead[86], C. Mora Herrera[49], A. Moraes[53], A. Morais[124a,b], N. Morange[136], J. Morel[54], G. Morello[36a,36b], D. Moreno[81], M. Moreno Llácer[167], P. Morettini[50a], M. Morii[57], J. Morin[75], Y. Morita[66], A.K. Morley[29], G. Mornacchi[29], M-C. Morone[49], S.V. Morozov[96], J.D. Morris[75], L. Morvaj[101], H.G. Moser[99], M. Mosidze[51], J. Moss[109], R. Mount[143], E. Mountricha[136], S.V. Mouraviev[94], E.J.W. Moyse[84], M. Mudrinic[12b], F. Mueller[58a], J. Mueller[123], K. Mueller[20], T.A. Müller[98], D. Muenstermann[29], A. Muijs[105], A. Muir[168], Y. Munwes[153], K. Murakami[66], W.J. Murray[129], I. Mussche[105], E. Musto[102a,102b], A.G. Myagkov[128], M. Myska[125], J. Nadal[11], K. Nagai[160], K. Nagano[66], Y. Nagasaka[60], A.M. Nairz[29], Y. Nakahama[29], K. Nakamura[155], I. Nakano[110], G. Nanava[20], A. Napier[161], M. Nash[77,c], N.R. Nation[21], T. Nattermann[20], T. Naumann[41], G. Navarro[162], H.A. Neal[87], E. Nebot[80], P.Yu. Nechaeva[94], A. Negri[119a,119b], G. Negri[29], S. Nektarijevic[49], A. Nelson[64], S. Nelson[143], T.K. Nelson[143], S. Nemecek[125], P. Nemethy[108], A.A. Nepomuceno[23a], M. Nessi[29,u], S.Y. Nesterov[121], M.S. Neubauer[165], A. Neusiedl[81], R.M. Neves[108], P. Nevski[24], P.R. Newman[17], R.B. Nickerson[118], R. Nicolaidou[136], L. Nicolas[139], B. Nicquevert[29], F. Niedercorn[115], J. Nielsen[137], T. Niinikoski[29], A. Nikiforov[15], V. Nikolaenko[128], K. Nikolaev[65], I. Nikolic-Audit[78], K. Nikolics[49], K. Nikolopoulos[24], H. Nilsen[48], P. Nilsson[7], Y. Ninomiya[155], A. Nisati[132a], T. Nishiyama[67], R. Nisius[99], L. Nodulman[5], M. Nomachi[116], I. Nomidis[154], M. Nordberg[29], B. Nordkvist[146a,146b], P.R. Norton[129], J. Novakova[126], M. Nozaki[66], M. Nožička[41], L. Nozka[113], I.M. Nugent[159a], A.-E. Nuncio-Quiroz[20], G. Nunes Hanninger[86], T. Nunnemann[98], E. Nurse[77], T. Nyman[29], B.J. O'Brien[45], S.W. O'Neale[17,*], D.C. O'Neil[142], V. O'Shea[53], F.G. Oakham[28,e], H. Oberlack[99], J. Ocariz[78], A. Ochi[67], S. Oda[155], S. Odaka[66], J. Odier[83], H. Ogren[61], A. Oh[82], S.H. Oh[44], C.C. Ohm[146a,146b], T. Ohshima[101], H. Ohshita[140], T.K. Ohska[66], T. Ohsugi[59], S. Okada[67], H. Okawa[163], Y. Okumura[101], T. Okuyama[155], M. Olcese[50a], A.G. Olchevski[65], M. Oliveira[124a,h], D. Oliveira Damazio[24], E. Oliver Garcia[167], D. Olivito[120], A. Olszewski[38], J. Olszowska[38], C. Omachi[67], A. Onofre[124a,v], P.U.E. Onyisi[30], C.J. Oram[159a], M.J. Oreglia[30], Y. Oren[153], D. Orestano[134a,134b], I. Orlov[107], C. Oropeza Barrera[53], R.S. Orr[158], B. Osculati[50a,50b], R. Ospanov[120],

C. Osuna[11], G. Otero y Garzon[26], J.P. Ottersbach[105], M. Ouchrif[135d], F. Ould-Saada[117], A. Ouraou[136], Q. Ouyang[32a], M. Owen[82], S. Owen[139], O.K. Øye[13], V.E. Ozcan[18a], N. Ozturk[7], A. Pacheco Pages[11], C. Padilla Aranda[11], E. Paganis[139], F. Paige[24], K. Pajchel[117], S. Palestini[29], D. Pallin[33], A. Palma[124a,b], J.D. Palmer[17], Y.B. Pan[172], E. Panagiotopoulou[9], B. Panes[31a], N. Panikashvili[87], S. Panitkin[24], D. Pantea[25a], M. Panuskova[125], V. Paolone[123], A. Papadelis[146a], Th.D. Papadopoulou[9], A. Paramonov[5], W. Park[24,w], M.A. Parker[27], F. Parodi[50a,50b], J.A. Parsons[34], U. Parzefall[48], E. Pasqualucci[132a], A. Passeri[134a], F. Pastore[134a,134b], Fr. Pastore[29], G. Pásztor[49,x], S. Pataraia[172], N. Patel[150], J.R. Pater[82], S. Patricelli[102a,102b], T. Pauly[29], M. Pecsy[144a], M.I. Pedraza Morales[172], S.V. Peleganchuk[107], H. Peng[172], R. Pengo[29], A. Penson[34], J. Penwell[61], M. Perantoni[23a], K. Perez[34,t], T. Perez Cavalcanti[41], E. Perez Codina[11], M.T. Pérez García-Estañ[167], V. Perez Reale[34], L. Perini[89a,89b], H. Pernegger[29], R. Perrino[72a], P. Perrodo[4], S. Persembe[3a], V.D. Peshekhonov[65], O. Peters[105], B.A. Petersen[29], J. Petersen[29], T.C. Petersen[35], E. Petit[83], A. Petridis[154], C. Petridou[154], E. Petrolo[132a], F. Petrucci[134a,134b], D. Petschull[41], M. Petteni[142], R. Pezoa[31b], A. Phan[86], A.W. Phillips[27], P.W. Phillips[129], G. Piacquadio[29], E. Piccaro[75], M. Piccinini[19a,19b], A. Pickford[53], S.M. Piec[41], R. Piegaia[26], J.E. Pilcher[30], A.D. Pilkington[82], J. Pina[124a,b], M. Pinamonti[164a,164c], A. Pinder[118], J.L. Pinfold[2], J. Ping[32c], B. Pinto[124a,b], O. Pirotte[29], C. Pizio[89a,89b], R. Placakyte[41], M. Plamondon[169], W.G. Plano[82], M.-A. Pleier[24], A.V. Pleskach[128], A. Poblaguev[24], A. Poddar[58a], F. Podlyski[33], L. Poggioli[115], T. Poghosyan[20], M. Pohl[49], F. Polci[55], G. Polesello[119a], A. Policicchio[138], A. Polini[19a], J. Poll[75], V. Polychronakos[24], D.M. Pomarede[136], D. Pomeroy[22], K. Pommès[29], L. Pontecorvo[132a], B.G. Pope[88], G.A. Popeneciu[25a], D.S. Popovic[12a], A. Poppleton[29], X. Portell Bueso[48], R. Porter[163], C. Posch[21], G.E. Pospelov[99], S. Pospisil[127], I.N. Potrap[99], C.J. Potter[149], C.T. Potter[114], G. Poulard[29], J. Poveda[172], R. Prabhu[77], P. Pralavorio[83], S. Prasad[57], R. Pravahan[7], S. Prell[64], K. Pretzl[16], L. Pribyl[29], D. Price[61], L.E. Price[5], M.J. Price[29], P.M. Prichard[73], D. Prieur[123], M. Primavera[72a], K. Prokofiev[108], F. Prokoshin[31b], S. Protopopescu[24], J. Proudfoot[5], X. Prudent[43], H. Przysiezniak[4], S. Psoroulas[20], E. Ptacek[114], J. Purdham[87], M. Purohit[24,w], P. Puzo[115], Y. Pylypchenko[117], J. Qian[87], Z. Qian[83], Z. Qin[41], A. Quadt[54], D.R. Quarrie[14], W.B. Quayle[172], F. Quinonez[31a], M. Raas[104], V. Radescu[58b], B. Radics[20], T. Rador[18a], F. Ragusa[89a,89b], G. Rahal[177], A.M. Rahimi[109], D. Rahm[24], S. Rajagopalan[24], M. Rammensee[48], M. Rammes[141], M. Ramstedt[146a,146b], K. Randrianarivony[28], P.N. Ratoff[71], F. Rauscher[98], E. Rauter[99], M. Raymond[29], A.L. Read[117], D.M. Rebuzzi[119a,119b], A. Redelbach[173], G. Redlinger[24], R. Reece[120], K. Reeves[40], A. Reichold[105], E. Reinherz-Aronis[153], A. Reinsch[114], I. Reisinger[42], D. Reljic[12a], C. Rembser[29], Z.L. Ren[151], A. Renaud[115], P. Renkel[39], M. Rescigno[132a], S. Resconi[89a], B. Resende[136], P. Reznicek[98], R. Rezvani[158], A. Richards[77], R. Richter[99], E. Richter-Was[38,y], M. Ridel[78], S. Rieke[81], M. Rijpstra[105], M. Rijssenbeek[148], A. Rimoldi[119a,119b], L. Rinaldi[19a], R.R. Rios[39], I. Riu[11], G. Rivoltella[89a,89b], F. Rizatdinova[112], E. Rizvi[75], S.H. Robertson[85,j], A. Robichaud-Veronneau[49], D. Robinson[27], J.E.M. Robinson[77], M. Robinson[114], A. Robson[53], J.G. Rocha de Lima[106], C. Roda[122a,122b], D. Roda Dos Santos[29], S. Rodier[80], D. Rodriguez[162], Y. Rodriguez Garcia[15], A. Roe[54], S. Roe[29], O. Røhne[117], V. Rojo[1], S. Rolli[161], A. Romaniouk[96], V.M. Romanov[65], G. Romeo[26], D. Romero Maltrana[31a], L. Roos[78], E. Ros[167], S. Rosati[132a,132b], K. Rosbach[49], M. Rose[76], G.A. Rosenbaum[158], E.I. Rosenberg[64], P.L. Rosendahl[13], L. Rosselet[49], V. Rossetti[11], E. Rossi[102a,102b], L.P. Rossi[50a], L. Rossi[89a,89b], M. Rotaru[25a], I. Roth[171], J. Rothberg[138], D. Rousseau[115], C.R. Royon[136], A. Rozanov[83], Y. Rozen[152], X. Ruan[115], I. Rubinskiy[41], B. Ruckert[98], N. Ruckstuhl[105], V.I. Rud[97], C. Rudolph[43], G. Rudolph[62], F. Rühr[6], F. Ruggieri[134a,134b], A. Ruiz-Martinez[64], E. Rulikowska-Zarebska[37], V. Rumiantsev[91,*], L. Rumyantsev[65], K. Runge[48], O. Runolfsson[20], Z. Rurikova[48], N.A. Rusakovich[65], D.R. Rust[61], J.P. Rutherfoord[6], C. Ruwiedel[14], P. Ruzicka[125], Y.F. Ryabov[121], V. Ryadovikov[128], P. Ryan[88], M. Rybar[126], G. Rybkin[115], N.C. Ryder[118], S. Rzaeva[10], A.F. Saavedra[150], I. Sadeh[153], H.F-W. Sadrozinski[137], R. Sadykov[65], F. Safai Tehrani[132a,132b], H. Sakamoto[155], G. Salamanna[75], A. Salamon[133a], M. Saleem[111], D. Salihagic[99], A. Salnikov[143], J. Salt[167], B.M. Salvachua Ferrando[5], D. Salvatore[36a,36b], F. Salvatore[149], A. Salvucci[104], A. Salzburger[29], D. Sampsonidis[154], B.H. Samset[117], A. Sanchez[102a,102b], H. Sandaker[13], H.G. Sander[81], M.P. Sanders[98], M. Sandhoff[174], T. Sandoval[27], R. Sandstroem[99], S. Sandvoss[174], D.P.C. Sankey[129], A. Sansoni[47], C. Santamarina Rios[85], C. Santoni[33], R. Santonico[133a,133b], H. Santos[124a], J.G. Saraiva[124a,b], T. Sarangi[172], E. Sarkisyan-Grinbaum[7], F. Sarri[122a,122b], G. Sartisohn[174], O. Sasaki[66], T. Sasaki[66], N. Sasao[68], I. Satsounkevitch[90], G. Sauvage[4], E. Sauvan[4], J.B. Sauvan[115], P. Savard[158,e], V. Savinov[123], D.O. Savu[29], P. Savva[9], L. Sawyer[24,l], D.H. Saxon[53], L.P. Says[33], C. Sbarra[19a,19b], A. Sbrizzi[19a,19b], O. Scallon[93], D.A. Scannicchio[163], J. Schaarschmidt[115], P. Schacht[99], U. Schäfer[81], S. Schaepe[20], S. Schaetzel[58b], A.C. Schaffer[115], D. Schaile[98], R.D. Schamberger[148], A.G. Schamov[107], V. Scharf[58a], V.A. Schegelsky[121], D. Scheirich[87], M.I. Scherzer[14], C. Schiavi[50a,50b], J. Schieck[98], M. Schioppa[36a,36b], S. Schlenker[29], J.L. Schlereth[5], E. Schmidt[48], K. Schmieden[20], C. Schmitt[81], S. Schmitt[58b], M. Schmitz[20], A. Schöning[58b], M. Schott[29], D. Schouten[142], J. Schovancova[125], M. Schram[85], C. Schroeder[81], N. Schroer[58c], S. Schuh[29], G. Schuler[29], J. Schultes[174], H.-C. Schultz-Coulon[58a], H. Schulz[15], J.W. Schumacher[20], M. Schumacher[48], B.A. Schumm[137], Ph. Schune[136], C. Schwanenberger[82], A. Schwartzman[143], Ph. Schwemling[78], R. Schwienhorst[88], R. Schwierz[43], J. Schwindling[136], W.G. Scott[129], J. Searcy[114], E. Sedykh[121], E. Segura[11], S.C. Seidel[103], A. Seiden[137], F. Seifert[43], J.M. Seixas[23a], G. Sekhniaidze[102a], D.M. Seliverstov[121], B. Sellden[146a], G. Sellers[73], M. Seman[144b],

N. Semprini-Cesari[19a,19b], C. Serfon[98], L. Serin[115], R. Seuster[99], H. Severini[111], M.E. Sevior[86], A. Sfyrla[29], E. Shabalina[54], M. Shamim[114], L.Y. Shan[32a], J.T. Shank[21], Q.T. Shao[86], M. Shapiro[14], P.B. Shatalov[95], L. Shaver[6], C. Shaw[53], K. Shaw[164a,164c], D. Sherman[175], P. Sherwood[77], A. Shibata[108], H. Shichi[101], S. Shimizu[29], M. Shimojima[100], T. Shin[56], A. Shmeleva[94], M.J. Shochet[30], D. Short[118], M.A. Shupe[6], P. Sicho[125], A. Sidoti[132a,132b], A. Siebel[174], F. Siegert[48], J. Siegrist[14], Dj. Sijacki[12a], O. Silbert[171], J. Silva[124a,b], Y. Silver[153], D. Silverstein[143], S.B. Silverstein[146a], V. Simak[127], O. Simard[136], Lj. Simic[12a], S. Simion[115], B. Simmons[77], M. Simonyan[35], P. Sinervo[158], N.B. Sinev[114], V. Sipica[141], G. Siragusa[173], A.N. Sisakyan[65], S.Yu. Sivoklokov[97], J. Sjölin[146a,146b], T.B. Sjursen[13], L.A. Skinnari[14], K. Skovpen[107], P. Skubic[111], N. Skvorodnev[22], M. Slater[17], T. Slavicek[127], K. Sliwa[161], T.J. Sloan[71], J. Sloper[29], V. Smakhtin[171], S.Yu. Smirnov[96], L.N. Smirnova[97], O. Smirnova[79], B.C. Smith[57], D. Smith[143], K.M. Smith[53], M. Smizanska[71], K. Smolek[127], A.A. Snesarev[94], S.W. Snow[82], J. Snow[111], J. Snuverink[105], S. Snyder[24], M. Soares[124a], R. Sobie[169,j], J. Sodomka[127], A. Soffer[153], C.A. Solans[167], M. Solar[127], J. Solc[127], E. Soldatov[96], U. Soldevila[167], E. Solfaroli Camillocci[132a,132b], A.A. Solodkov[128], O.V. Solovyanov[128], J. Sondericker[24], N. Soni[2], V. Sopko[127], B. Sopko[127], M. Sorbi[89a,89b], M. Sosebee[7], A. Soukharev[107], S. Spagnolo[72a,72b], F. Spanò[34], R. Spighi[19a], G. Spigo[29], F. Spila[132a,132b], E. Spiriti[134a], R. Spiwoks[29], M. Spousta[126], T. Spreitzer[158], B. Spurlock[7], R.D.St. Denis[53], T. Stahl[141], J. Stahlman[120], R. Stamen[58a], E. Stanecka[29], R.W. Stanek[5], C. Stanescu[134a], S. Stapnes[117], E.A. Starchenko[128], J. Stark[55], P. Staroba[125], P. Starovoitov[91], A. Staude[98], P. Stavina[144a], G. Stavropoulos[14], G. Steele[53], P. Steinbach[43], P. Steinberg[24], I. Stekl[127], B. Stelzer[142], H.J. Stelzer[41], O. Stelzer-Chilton[159a], H. Stenzel[52], K. Stevenson[75], G.A. Stewart[29], J.A. Stillings[20], T. Stockmanns[20], M.C. Stockton[29], K. Stoerig[48], G. Stoicea[25a], S. Stonjek[99], P. Strachota[126], A.R. Stradling[7], A. Straessner[43], J. Strandberg[147], S. Strandberg[146a,146b], A. Strandlie[117], M. Strang[109], E. Strauss[143], M. Strauss[111], P. Strizenec[144b], R. Ströhmer[173], D.M. Strom[114], J.A. Strong[76,*], R. Stroynowski[39], J. Strube[129], B. Stugu[13], I. Stumer[24,*], J. Stupak[148], P. Sturm[174], D.A. Soh[151,q], D. Su[143], H.S. Subramania[2], A. Succurro[11], Y. Sugaya[116], T. Sugimoto[101], C. Suhr[106], K. Suita[67], M. Suk[126], V.V. Sulin[94], S. Sultansoy[3d], T. Sumida[29], X. Sun[55], J.E. Sundermann[48], K. Suruliz[139], S. Sushkov[11], G. Susinno[36a,36b], M.R. Sutton[149], Y. Suzuki[66], M. Svatos[125], Yu.M. Sviridov[128], S. Swedish[168], I. Sykora[144a], T. Sykora[126], B. Szeless[29], J. Sánchez[167], D. Ta[105], K. Tackmann[41], A. Taffard[163], R. Tafirout[159a], A. Taga[117], N. Taiblum[153], Y. Takahashi[101], H. Takai[24], R. Takashima[69], H. Takeda[67], T. Takeshita[140], M. Talby[83], A. Talyshev[107], M.C. Tamsett[24], J. Tanaka[155], R. Tanaka[115], S. Tanaka[131], S. Tanaka[66], Y. Tanaka[100], K. Tani[67], N. Tannoury[83], G.P. Tappern[29], S. Tapprogge[81], D. Tardif[158], S. Tarem[152], F. Tarrade[24], G.F. Tartarelli[89a], P. Tas[126], M. Tasevsky[125], E. Tassi[36a,36b], M. Tatarkhanov[14], C. Taylor[77], F.E. Taylor[92], G.N. Taylor[86], W. Taylor[159b], M. Teixeira Dias Castanheira[75], P. Teixeira-Dias[76], K.K. Temming[48], H. Ten Kate[29], P.K. Teng[151], S. Terada[66], K. Terashi[155], J. Terron[80], M. Terwort[41,o], M. Testa[47], R.J. Teuscher[158,j], J. Thadome[174], J. Therhaag[20], T. Theveneaux-Pelzer[78], M. Thioye[175], S. Thoma[48], J.P. Thomas[17], E.N. Thompson[84], P.D. Thompson[17], P.D. Thompson[158], A.S. Thompson[53], E. Thomson[120], M. Thomson[27], R.P. Thun[87], T. Tic[125], V.O. Tikhomirov[94], Y.A. Tikhonov[107], C.J.W.P. Timmermans[104], P. Tipton[175], F.J. Tique Aires Viegas[29], S. Tisserant[83], J. Tobias[48], B. Toczek[37], T. Todorov[4], S. Todorova-Nova[161], B. Toggerson[163], J. Tojo[66], S. Tokár[144a], K. Tokunaga[67], K. Tokushuku[66], K. Tollefson[88], M. Tomoto[101], L. Tompkins[14], K. Toms[103], G. Tong[32a], A. Tonoyan[13], C. Topfel[16], N.D. Topilin[65], I. Torchiani[29], E. Torrence[114], H. Torres[78], E. Torró Pastor[167], J. Toth[83,x], F. Touchard[83], D.R. Tovey[139], D. Traynor[75], T. Trefzger[173], L. Tremblet[29], A. Tricoli[29], I.M. Trigger[159a], S. Trincaz-Duvoid[78], T.N. Trinh[78], M.F. Tripiana[70], W. Trischuk[158], A. Trivedi[24,w], B. Trocmé[55], C. Troncon[89a], M. Trottier-McDonald[142], A. Trzupek[38], C. Tsarouchas[29], J.C-L. Tseng[118], M. Tsiakiris[105], P.V. Tsiareshka[90], D. Tsionou[4], G. Tsipolitis[9], V. Tsiskaridze[48], E.G. Tskhadadze[51], I.I. Tsukerman[95], V. Tsulaia[123], J.-W. Tsung[20], S. Tsuno[66], D. Tsybychev[148], A. Tua[139], J.M. Tuggle[30], M. Turala[38], D. Turecek[127], I. Turk Cakir[3e], E. Turlay[105], R. Turra[89a,89b], P.M. Tuts[34], A. Tykhonov[74], M. Tylmad[146a,146b], M. Tyndel[129], H. Tyrvainen[29], G. Tzanakos[8], K. Uchida[20], I. Ueda[155], R. Ueno[28], M. Ugland[13], M. Uhlenbrock[20], M. Uhrmacher[54], F. Ukegawa[160], G. Unal[29], D.G. Underwood[5], A. Undrus[24], G. Unel[163], Y. Unno[66], D. Urbaniec[34], E. Urkovsky[153], P. Urrejola[31a], G. Usai[7], M. Uslenghi[119a,119b], L. Vacavant[83], V. Vacek[127], B. Vachon[85], S. Vahsen[14], J. Valenta[125], P. Valente[132a], S. Valentinetti[19a,19b], S. Valkar[126], E. Valladolid Gallego[167], S. Vallecorsa[152], J.A. Valls Ferrer[167], H. van der Graaf[105], E. van der Kraaij[105], R. Van Der Leeuw[105], E. van der Poel[105], D. van der Ster[29], B. Van Eijk[105], N. van Eldik[84], P. van Gemmeren[5], Z. van Kesteren[105], I. van Vulpen[105], W. Vandelli[29], G. Vandoni[29], A. Vaniachine[5], P. Vankov[41], F. Vannucci[78], F. Varela Rodriguez[29], R. Vari[132a], E.W. Varnes[6], D. Varouchas[14], A. Vartapetian[7], K.E. Varvell[150], V.I. Vassilakopoulos[56], F. Vazeille[33], G. Vegni[89a,89b], J.J. Veillet[115], C. Vellidis[8], F. Veloso[124a], R. Veness[29], S. Veneziano[132a], A. Ventura[72a,72b], D. Ventura[138], M. Venturi[48], N. Venturi[16], V. Vercesi[119a], M. Verducci[138], W. Verkerke[105], J.C. Vermeulen[105], A. Vest[43], M.C. Vetterli[142,e], I. Vichou[165], T. Vickey[145b,z], G.H.A. Viehhauser[118], S. Viel[168], M. Villa[19a,19b], M. Villaplana Perez[167], E. Vilucchi[47], M.G. Vincter[28], E. Vinek[29], V.B. Vinogradov[65], M. Virchaux[136,*], J. Virzi[14], O. Vitells[171], M. Viti[41], I. Vivarelli[48], F. Vives Vaque[11], S. Vlachos[9], M. Vlasak[127], N. Vlasov[20], A. Vogel[20], P. Vokac[127], G. Volpi[47], M. Volpi[11], G. Volpini[89a], H. von der Schmitt[99], J. von Loeben[99], H. von Radziewski[48], E. von Toerne[20], V. Vorobel[126], A.P. Vorobiev[128], V. Vorwerk[11], M. Vos[167], R. Voss[29], T.T. Voss[174], J.H. Vossebeld[73], N. Vranjes[12a], M. Vranjes Milosavljevic[12a],

V. Vrba[125], M. Vreeswijk[105], T. Vu Anh[81], R. Vuillermet[29], I. Vukotic[115], W. Wagner[174], P. Wagner[120], H. Wahlen[174], J. Wakabayashi[101], J. Walbersloh[42], S. Walch[87], J. Walder[71], R. Walker[98], W. Walkowiak[141], R. Wall[175], P. Waller[73], C. Wang[44], H. Wang[172], H. Wang[32b,aa], J. Wang[151], J. Wang[32d], J.C. Wang[138], R. Wang[103], S.M. Wang[151], A. Warburton[85], C.P. Ward[27], M. Warsinsky[48], P.M. Watkins[17], A.T. Watson[17], M.F. Watson[17], G. Watts[138], S. Watts[82], A.T. Waugh[150], B.M. Waugh[77], J. Weber[42], M. Weber[129], M.S. Weber[16], P. Weber[54], A.R. Weidberg[118], P. Weigell[99], J. Weingarten[54], C. Weiser[48], H. Wellenstein[22], P.S. Wells[29], M. Wen[47], T. Wenaus[24], S. Wendler[123], Z. Weng[151,q], T. Wengler[29], S. Wenig[29], N. Wermes[20], M. Werner[48], P. Werner[29], M. Werth[163], M. Wessels[58a], C. Weydert[55], K. Whalen[28], S.J. Wheeler-Ellis[163], S.P. Whitaker[21], A. White[7], M.J. White[86], S. White[24], S.R. Whitehead[118], D. Whiteson[163], D. Whittington[61], F. Wicek[115], D. Wicke[174], F.J. Wickens[129], W. Wiedenmann[172], M. Wielers[129], P. Wienemann[20], C. Wiglesworth[75], L.A.M. Wiik[48], P.A. Wijeratne[77], A. Wildauer[167], M.A. Wildt[41,o], I. Wilhelm[126], H.G. Wilkens[29], J.Z. Will[98], E. Williams[34], H.H. Williams[120], W. Willis[34], S. Willocq[84], J.A. Wilson[17], M.G. Wilson[143], A. Wilson[87], I. Wingerter-Seez[4], S. Winkelmann[48], F. Winklmeier[29], M. Wittgen[143], M.W. Wolter[38], H. Wolters[124a,h], G. Wooden[118], B.K. Wosiek[38], J. Wotschack[29], M.J. Woudstra[84], K. Wraight[53], C. Wright[53], B. Wrona[73], S.L. Wu[172], X. Wu[49], Y. Wu[32b,ab], E. Wulf[34], R. Wunstorf[42], B.M. Wynne[45], L. Xaplanteris[9], S. Xella[35], S. Xie[48], Y. Xie[32a], C. Xu[32b,ac], D. Xu[139], G. Xu[32a], B. Yabsley[150], M. Yamada[66], A. Yamamoto[66], K. Yamamoto[64], S. Yamamoto[155], T. Yamamura[155], J. Yamaoka[44], T. Yamazaki[155], Y. Yamazaki[67], Z. Yan[21], H. Yang[87], U.K. Yang[82], Y. Yang[61], Y. Yang[32a], Z. Yang[146a,146b], S. Yanush[91], W-M. Yao[14], Y. Yao[14], Y. Yasu[66], G.V. Ybeles Smit[130], J. Ye[39], S. Ye[24], M. Yilmaz[3c], R. Yoosoofmiya[123], K. Yorita[170], R. Yoshida[5], C. Young[143], S. Youssef[21], D. Yu[24], J. Yu[7], J. Yu[32c,ac], L. Yuan[32a,ad], A. Yurkewicz[148], V.G. Zaets[128], R. Zaidan[63], A.M. Zaitsev[128], Z. Zajacova[29], Yo.K. Zalite[121], L. Zanello[132a,132b], P. Zarzhitsky[39], A. Zaytsev[107], C. Zeitnitz[174], M. Zeller[175], A. Zemla[38], C. Zendler[20], A.V. Zenin[128], O. Zenin[128], T. Ženiš[144a], Z. Zenonos[122a,122b], S. Zenz[14], D. Zerwas[115], G. Zevi della Porta[57], Z. Zhan[32d], D. Zhang[32b,aa], H. Zhang[88], J. Zhang[5], X. Zhang[32d], Z. Zhang[115], L. Zhao[108], T. Zhao[138], Z. Zhao[32b], A. Zhemchugov[65], S. Zheng[32a], J. Zhong[151,ae], B. Zhou[87], N. Zhou[163], Y. Zhou[151], C.G. Zhu[32d], H. Zhu[41], J. Zhu[87], Y. Zhu[172], X. Zhuang[98], V. Zhuravlov[99], D. Zieminska[61], R. Zimmermann[20], S. Zimmermann[20], S. Zimmermann[48], M. Ziolkowski[141], R. Zitoun[4], L. Živković[34], V.V. Zmouchko[128,*], G. Zobernig[172], A. Zoccoli[19a,19b], Y. Zolnierowski[4], A. Zsenei[29], M. zur Nedden[15], V. Zutshi[106], L. Zwalinski[29]

[1] University at Albany, Albany, NY, United States of America

[2] Department of Physics, University of Alberta, Edmonton, AB, Canada

[3] (a) Department of Physics, Ankara University, Ankara; (b) Department of Physics, Dumlupinar University, Kutahya; (c) Department of Physics, Gazi University, Ankara; (d) Division of Physics, TOBB University of Economics and Technology, Ankara; (e) Turkish Atomic Energy Authority, Ankara, Turkey

[4] LAPP, CNRS/IN2P3 and Université de Savoie, Annecy-le-Vieux, France

[5] High Energy Physics Division, Argonne National Laboratory, Argonne, IL, United States of America

[6] Department of Physics, University of Arizona, Tucson, AZ, United States of America

[7] Department of Physics, The University of Texas at Arlington, Arlington, TX, United States of America

[8] Physics Department, University of Athens, Athens, Greece

[9] Physics Department, National Technical University of Athens, Zografou, Greece

[10] Institute of Physics, Azerbaijan Academy of Sciences, Baku, Azerbaijan

[11] Institut de Física d'Altes Energies, Universitat Autònoma de Barcelona and ICREA, Barcelona, Spain

[12] (a) Institute of Physics, University of Belgrade, Belgrade; (b) Vinca Institute of Nuclear Sciences, Belgrade, Serbia

[13] Department for Physics and Technology, University of Bergen, Bergen, Norway

[14] Physics Division, Lawrence Berkeley National Laboratory and University of California, Berkeley, CA, United States of America

[15] Department of Physics, Humboldt University, Berlin, Germany

[16] Albert Einstein Center for Fundamental Physics and Laboratory for High Energy Physics, University of Bern, Bern, Switzerland

[17] School of Physics and Astronomy, University of Birmingham, Birmingham, United Kingdom

[18] (a) Department of Physics, Bogazici University, Istanbul; (b) Division of Physics, Dogus University, Istanbul; (c) Department of Physics Engineering, Gaziantep University, Gaziantep; (d) Department of Physics, Istanbul Technical University, Istanbul, Turkey

[19] (a) INFN Sezione di Bologna; (b) Dipartimento di Fisica, Università di Bologna, Bologna, Italy

[20] Physikalisches Institut, University of Bonn, Bonn, Germany

[21] Department of Physics, Boston University, Boston, MA, United States of America

[22] Department of Physics, Brandeis University, Waltham, MA, United States of America

[23](a)Universidade Federal do Rio De Janeiro COPPE/EE/IF, Rio de Janeiro; (b)Instituto de Fisica, Universidade de Sao Paulo, Sao Paulo, Brazil

[24]Physics Department, Brookhaven National Laboratory, Upton, NY, United States of America

[25](a)National Institute of Physics and Nuclear Engineering, Bucharest; (b)University Politehnica Bucharest, Bucharest; (c)West University in Timisoara, Timisoara, Romania

[26]Departamento de Física, Universidad de Buenos Aires, Buenos Aires, Argentina

[27]Cavendish Laboratory, University of Cambridge, Cambridge, United Kingdom

[28]Department of Physics, Carleton University, Ottawa, ON, Canada

[29]CERN, Geneva, Switzerland

[30]Enrico Fermi Institute, University of Chicago, Chicago, IL, United States of America

[31](a)Departamento de Fisica, Pontificia Universidad Cat ólica de Chile, Santiago; (b)Departamento de Física, Universidad Técnica Federico Santa María, Valparaíso, Chile

[32](a)Institute of High Energy Physics, Chinese Academy of Sciences, Beijing; (b)Department of Modern Physics, University of Science and Technology of China, Anhui; (c)Department of Physics, Nanjing University, Jiangsu; (d)High Energy Physics Group, Shandong University, Shandong, China

[33]Laboratoire de Physique Corpusculaire, Clermont Université and Université Blaise Pascal and CNRS/IN2P3, Aubiere Cedex, France

[34]Nevis Laboratory, Columbia University, Irvington, NY, United States of America

[35]Niels Bohr Institute, University of Copenhagen, Kobenhavn, Denmark

[36](a)INFN Gruppo Collegato di Cosenza; (b)Dipartimento di Fisica, Università della Calabria, Arcavata di Rende, Italy

[37]Faculty of Physics and Applied Computer Science, AGH-University of Science and Technology, Krakow, Poland

[38]The Henryk Niewodniczanski Institute of Nuclear Physics, Polish Academy of Sciences, Krakow, Poland

[39]Physics Department, Southern Methodist University, Dallas, TX, United States of America

[40]Physics Department, University of Texas at Dallas, Richardson, TX, United States of America

[41]DESY, Hamburg and Zeuthen, Germany

[42]Institut für Experimentelle Physik IV, Technische Universität Dortmund, Dortmund, Germany

[43]Institut für Kern- und Teilchenphysik, Technical University Dresden, Dresden, Germany

[44]Department of Physics, Duke University, Durham, NC, United States of America

[45]SUPA - School of Physics and Astronomy, University of Edinburgh, Edinburgh, United Kingdom

[46]Johannes Gutenbergstrasse 3 2700 Wiener Neustadt, Austria

[47]INFN Laboratori Nazionali di Frascati, Frascati, Italy

[48]Fakultät für Mathematik und Physik, Albert-Ludwigs-Universität, Freiburg i.Br., Germany

[49]Section de Physique, Université de Genève, Geneva, Switzerland

[50](a)INFN Sezione di Genova; (b)Dipartimento di Fisica, Università di Genova, Genova, Italy

[51]Institute of Physics and HEP Institute, Georgian Academy of Sciences and Tbilisi State University, Tbilisi, Georgia

[52]II Physikalisches Institut, Justus-Liebig-Universität Giessen, Giessen, Germany

[53]SUPA - School of Physics and Astronomy, University of Glasgow, Glasgow, United Kingdom

[54]II Physikalisches Institut, Georg-August-Universität, Göttingen, Germany

[55]Laboratoire de Physique Subatomique et de Cosmologie, Université Joseph Fourier and CNRS/IN2P3 and Institut National Polytechnique de Grenoble, Grenoble, France

[56]Department of Physics, Hampton University, Hampton, VA, United States of America

[57]Laboratory for Particle Physics and Cosmology, Harvard University, Cambridge, MA, United States of America

[58](a)Kirchhoff-Institut für Physik, Ruprecht-Karls-Universität Heidelberg, Heidelberg; (b)Physikalisches Institut, Ruprecht-Karls-Universit ät Heidelberg, Heidelberg; (c)ZITI Institut für technische Informatik, Ruprecht-Karls-Universität Heidelberg, Mannheim, Germany

[59]Faculty of Science, Hiroshima University, Hiroshima, Japan

[60]Faculty of Applied Information Science, Hiroshima Institute of Technology, Hiroshima, Japan

[61]Department of Physics, Indiana University, Bloomington, IN, United States of America

[62]Institut für Astro- und Teilchenphysik, Leopold-Franzens-Universität, Innsbruck, Austria

[63]University of Iowa, Iowa City, IA, United States of America

[64]Department of Physics and Astronomy, Iowa State University, Ames, IA, United States of America

[65]Joint Institute for Nuclear Research, JINR Dubna, Dubna, Russia

[66]KEK, High Energy Accelerator Research Organization, Tsukuba, Japan

[67]Graduate School of Science, Kobe University, Kobe, Japan

[68]Faculty of Science, Kyoto University, Kyoto, Japan

[69]Kyoto University of Education, Kyoto, Japan

[70]Instituto de Física La Plata, Universidad Nacional de La Plata and CONICET, La Plata, Argentina

[71]Physics Department, Lancaster University, Lancaster, United Kingdom

[72](a)INFN Sezione di Lecce; (b)Dipartimento di Fisica, Università del Salento, Lecce, Italy

[73]Oliver Lodge Laboratory, University of Liverpool, Liverpool, United Kingdom

[74]Department of Physics, Jožef Stefan Institute and University of Ljubljana, Ljubljana, Slovenia

[75]Department of Physics, Queen Mary University of London, London, United Kingdom

[76]Department of Physics, Royal Holloway University of London, Surrey, United Kingdom

[77]Department of Physics and Astronomy, University College London, London, United Kingdom

[78]Laboratoire de Physique Nucléaire et de Hautes Energies, UPMC and Université Paris-Diderot and CNRS/IN2P3, Paris, France

[79]Fysiska institutionen, Lunds universitet, Lund, Sweden

[80]Departamento de Fisica Teorica C-15, Universidad Autonoma de Madrid, Madrid, Spain

[81]Institut für Physik, Universit ät Mainz, Mainz, Germany

[82]School of Physics and Astronomy, University of Manchester, Manchester, United Kingdom

[83]CPPM, Aix-Marseille Université and CNRS/IN2P3, Marseille, France

[84]Department of Physics, University of Massachusetts, Amherst, MA, United States of America

[85]Department of Physics, McGill University, Montreal, QC, Canada

[86]School of Physics, University of Melbourne, Victoria, Australia

[87]Department of Physics, The University of Michigan, Ann Arbor, MI, United States of America

[88]Department of Physics and Astronomy, Michigan State University, East Lansing, MI, United States of America

[89](a)INFN Sezione di Milano; (b)Dipartimento di Fisica, Università di Milano, Milano, Italy

[90]B.I. Stepanov Institute of Physics, National Academy of Sciences of Belarus, Minsk, Republic of Belarus

[91]National Scientific and Educational Centre for Particle and High Energy Physics, Minsk, Republic of Belarus

[92]Department of Physics, Massachusetts Institute of Technology, Cambridge, MA, United States of America

[93]Group of Particle Physics, University of Montreal, Montreal, QC, Canada

[94]P.N. Lebedev Institute of Physics, Academy of Sciences, Moscow, Russia

[95]Institute for Theoretical and Experimental Physics (ITEP), Moscow, Russia

[96]Moscow Engineering and Physics Institute (MEPhI), Moscow, Russia

[97]Skobeltsyn Institute of Nuclear Physics, Lomonosov Moscow State University, Moscow, Russia

[98]Fakultät für Physik, Ludwig-Maximilians-Universität München, M ünchen, Germany

[99]Max-Planck-Institut für Physik (Werner-Heisenberg-Institut), München, Germany

[100]Nagasaki Institute of Applied Science, Nagasaki, Japan

[101]Graduate School of Science, Nagoya University, Nagoya, Japan

[102](a)INFN Sezione di Napoli; (b)Dipartimento di Scienze Fisiche, Università di Napoli, Napoli, Italy

[103]Department of Physics and Astronomy, University of New Mexico, Albuquerque, NM, United States of America

[104]Institute for Mathematics, Astrophysics and Particle Physics, Radboud University Nijmegen/Nikhef, Nijmegen, Netherlands

[105]Nikhef National Institute for Subatomic Physics and University of Amsterdam, Amsterdam, Netherlands

[106]Department of Physics, Northern Illinois University, DeKalb, IL, United States of America

[107]Budker Institute of Nuclear Physics (BINP), Novosibirsk, Russia

[108]Department of Physics, New York University, New York, NY, United States of America

[109]Ohio State University, Columbus, OH, United States of America

[110]Faculty of Science, Okayama University, Okayama, Japan

[111]Homer L. Dodge Department of Physics and Astronomy, University of Oklahoma, Norman, OK, United States of America

[112]Department of Physics, Oklahoma State University, Stillwater, OK, United States of America

[113]Palacký University, RCPTM, Olomouc, Czech Republic

[114]Center for High Energy Physics, University of Oregon, Eugene, OR, United States of America

[115]LAL, Univ. Paris-Sud and CNRS/IN2P3, Orsay, France

[116]Graduate School of Science, Osaka University, Osaka, Japan

[117]Department of Physics, University of Oslo, Oslo, Norway

[118]Department of Physics, Oxford University, Oxford, United Kingdom

[119](a)INFN Sezione di Pavia; (b)Dipartimento di Fisica Nucleare e Teorica, Università di Pavia, Pavia, Italy

[120]Department of Physics, University of Pennsylvania, Philadelphia, PA, United States of America

[121]Petersburg Nuclear Physics Institute, Gatchina, Russia

[122](a)INFN Sezione di Pisa; (b)Dipartimento di Fisica E. Fermi, Università di Pisa, Pisa, Italy

[123]Department of Physics and Astronomy, University of Pittsburgh, Pittsburgh, PA, United States of America

[124](a)Laboratorio de Instrumentacao e Fisica Experimental de Particulas - LIP, Lisboa, Portugal; (b)Departamento de Fisica Teorica y del Cosmos and CAFPE, Universidad de Granada, Granada, Spain

[125]Institute of Physics, Academy of Sciences of the Czech Republic, Praha, Czech Republic

[126]Faculty of Mathematics and Physics, Charles University in Prague, Praha, Czech Republic

[127]Czech Technical University in Prague, Praha, Czech Republic

[128]State Research Center Institute for High Energy Physics, Protvino, Russia

[129]Particle Physics Department, Rutherford Appleton Laboratory, Didcot, United Kingdom

[130]Physics Department, University of Regina, Regina, SK, Canada

[131]Ritsumeikan University, Kusatsu, Shiga, Japan

[132](a)INFN Sezione di Roma I; (b)Dipartimento di Fisica, Università La Sapienza, Roma, Italy

[133](a)INFN Sezione di Roma Tor Vergata; (b)Dipartimento di Fisica, Università di Roma Tor Vergata, Roma, Italy

[134](a)INFN Sezione di Roma Tre; (b)Dipartimento di Fisica, Università Roma Tre, Roma, Italy

[135](a)Faculté des Sciences Ain Chock, Réseau Universitaire de Physique des Hautes Energies - Université Hassan II, Casablanca; (b)Centre National de l'Energie des Sciences Techniques Nucleaires, Rabat; (c)Université Cadi Ayyad, Faculté des sciences Semlalia Département de Physique, B.P. 2390 Marrakech 40000; (d)Faculté des Sciences, Université Mohamed Premier and LPTPM, Oujda; (e)Faculté des Sciences, Université Mohammed V, Rabat, Morocco

[136]DSM/IRFU (Institut de Recherches sur les Lois Fondamentales de l'Univers), CEA Saclay (Commissariat a l'Energie Atomique), Gif-sur-Yvette, France

[137]Santa Cruz Institute for Particle Physics, University of California Santa Cruz, Santa Cruz, CA, United States of America

[138]Department of Physics, University of Washington, Seattle, WA, United States of America

[139]Department of Physics and Astronomy, University of Sheffield, Sheffield, United Kingdom

[140]Department of Physics, Shinshu University, Nagano, Japan

[141]Fachbereich Physik, Universit ät Siegen, Siegen, Germany

[142]Department of Physics, Simon Fraser University, Burnaby, BC, Canada

[143]SLAC National Accelerator Laboratory, Stanford, CA, United States of America

[144](a)Faculty of Mathematics, Physics & Informatics, Comenius University, Bratislava; (b)Department of Subnuclear Physics, Institute of Experimental Physics of the Slovak Academy of Sciences, Kosice, Slovak Republic

[145](a)Department of Physics, University of Johannesburg, Johannesburg; (b)School of Physics, University of the Witwatersrand, Johannesburg, South Africa

[146](a)Department of Physics, Stockholm University; (b)The Oskar Klein Centre, Stockholm, Sweden

[147]Physics Department, Royal Institute of Technology, Stockholm, Sweden

[148]Department of Physics and Astronomy, Stony Brook University, Stony Brook, NY, United States of America

[149]Department of Physics and Astronomy, University of Sussex, Brighton, United Kingdom

[150]School of Physics, University of Sydney, Sydney, Australia

[151]Institute of Physics, Academia Sinica, Taipei, Taiwan

[152]Department of Physics, Technion: Israel Inst. of Technology, Haifa, Israel

[153]Raymond and Beverly Sackler School of Physics and Astronomy, Tel Aviv University, Tel Aviv, Israel

[154]Department of Physics, Aristotle University of Thessaloniki, Thessaloniki, Greece

[155]International Center for Elementary Particle Physics and Department of Physics, The University of Tokyo, Tokyo, Japan

[156]Graduate School of Science and Technology, Tokyo Metropolitan University, Tokyo, Japan

[157]Department of Physics, Tokyo Institute of Technology, Tokyo, Japan

[158]Department of Physics, University of Toronto, Toronto, ON, Canada

[159](a)TRIUMF, Vancouver, BC; (b)Department of Physics and Astronomy, York University, Toronto, ON, Canada

[160]Institute of Pure and Applied Sciences, University of Tsukuba, Ibaraki, Japan

[161]Science and Technology Center, Tufts University, Medford, MA, United States of America

[162]Centro de Investigaciones, Universidad Antonio Narino, Bogota, Colombia

^{163}Department of Physics and Astronomy, University of California Irvine, Irvine, CA, United States of America

^{164}(a)INFN Gruppo Collegato di Udine; (b)ICTP, Trieste; (c)Dipartimento di Fisica, Università di Udine, Udine, Italy

^{165}Department of Physics, University of Illinois, Urbana, IL, United States of America

^{166}Department of Physics and Astronomy, University of Uppsala, Uppsala, Sweden

^{167}Instituto de Física Corpuscular (IFIC) and Departamento de Física Atómica, Molecular y Nuclear and Departamento de Ingenierá Electrónica and Instituto de Microelectrónica de Barcelona (IMB-CNM), University of Valencia and CSIC, Valencia, Spain

^{168}Department of Physics, University of British Columbia, Vancouver, BC, Canada

^{169}Department of Physics and Astronomy, University of Victoria, Victoria, BC, Canada

^{170}Waseda University, Tokyo, Japan

^{171}Department of Particle Physics, The Weizmann Institute of Science, Rehovot, Israel

^{172}Department of Physics, University of Wisconsin, Madison, WI, United States of America

^{173}Fakultät für Physik und Astronomie, Julius-Maximilians-Universität, Würzburg, Germany

^{174}Fachbereich C Physik, Bergische Universität Wuppertal, Wuppertal, Germany

^{175}Department of Physics, Yale University, New Haven, CT, United States of America

^{176}Yerevan Physics Institute, Yerevan, Armenia

^{177}Domaine scientifique de la Doua, Centre de Calcul CNRS/IN2P3, Villeurbanne Cedex, France

^{a}Also at Laboratorio de Instrumentacao e Fisica Experimental de Particulas - LIP, Lisboa, Portugal

^{b}Also at Faculdade de Ciencias and CFNUL, Universidade de Lisboa, Lisboa, Portugal

^{c}Also at Particle Physics Department, Rutherford Appleton Laboratory, Didcot, United Kingdom

^{d}Also at CPPM, Aix-Marseille Université and CNRS/IN2P3, Marseille, France

^{e}Also at TRIUMF, Vancouver, BC, Canada

^{f}Also at Department of Physics, California State University, Fresno, CA, United States of America

^{g}Also at Faculty of Physics and Applied Computer Science, AGH-University of Science and Technology, Krakow, Poland

^{h}Also at Department of Physics, University of Coimbra, Coimbra, Portugal

^{i}Also at Università di Napoli Parthenope, Napoli, Italy

^{j}Also at Institute of Particle Physics (IPP), Canada

^{k}Also at Department of Physics, Middle East Technical University, Ankara, Turkey

^{l}Also at Louisiana Tech University, Ruston, LA, United States of America

^{m}Also at Group of Particle Physics, University of Montreal, Montreal, QC, Canada

^{n}Also at Institute of Physics, Azerbaijan Academy of Sciences, Baku, Azerbaijan

^{o}Also at Institut für Experimentalphysik, Universität Hamburg, Hamburg, Germany

^{p}Also at Manhattan College, New York, NY, United States of America

^{q}Also at School of Physics and Engineering, Sun Yat-sen University, Guanzhou, China

^{r}Also at Academia Sinica Grid Computing, Institute of Physics, Academia Sinica, Taipei, Taiwan

^{s}Also at High Energy Physics Group, Shandong University, Shandong, China

^{t}Also at California Institute of Technology, Pasadena, CA, United States of America

^{u}Also at Section de Physique, Université de Genève, Geneva, Switzerland

^{v}Also at Departamento de Fisica, Universidade de Minho, Braga, Portugal

^{w}Also at Department of Physics and Astronomy, University of South Carolina, Columbia, SC, United States of America

^{x}Also at KFKI Research Institute for Particle and Nuclear Physics, Budapest, Hungary

^{y}Also at Institute of Physics, Jagiellonian University, Krakow, Poland

^{z}Also at Department of Physics, Oxford University, Oxford, United Kingdom

^{aa}Also at Institute of Physics, Academia Sinica, Taipei, Taiwan

^{ab}Also at Department of Physics, The University of Michigan, Ann Arbor MI, United States of America

^{ac}Also at DSM/IRFU (Institut de Recherches sur les Lois Fondamentales de l'Univers), CEA Saclay (Commissariat a l'Energie Atomique), Gif-sur-Yvette, France

^{ad}Also at Laboratoire de Physique Nucléaire et de Hautes Energies, UPMC and Université Paris-Diderot and CNRS/IN2P3, Paris, France

^{ae}Also at Department of Physics, Nanjing University, Jiangsu, China

*Deceased